Saltwater Intrusion in Fractured Crystalline Bedrock Aquifer - A Case Study on Koster Islands, SW Sweden

Sibhat Afewerki

Degree of Master of Science (120 credits)
with a major in Earth Sciences
45 hec

Department of Earth Sciences
University of Gothenburg
2019 B1069

Faculty of Science

UNIVERSITY OF GOTHENBURG

UNIVERSITY OF GOTHENBURG
Department of Earth Sciences
Geovetarcentrum/Earth Science Centre

Saltwater Intrusion in Fractured Crystalline Bedrock Aquifer - A Case Study on Koster Islands, SW Sweden

Sibhat Afewerki

ISSN 1400-3821

B1069
Master of Science (120 credits) thesis
Göteborg 2019

Mailing address
Geovetarcentrum
S 405 30 Göteborg

Address
Geovetarcentrum
Guldhedsgatan 5A

Telephone
031-786 19 56

Geovetarcentrum
Göteborg University
S-405 30 Göteborg
SWEDEN

Abstract

Saltwater intrusion (SWI) is one of the significant threats in many coastal areas, mainly driven by anthropogenic hazards (over-pumping) and climate change (sea level rise). So far, there have been extensive research and techniques to understand and minimize SWI. However, quantification and mechanism of SWI remain unclear and incomplete, especially in fractured crystalline bedrock aquifer.

This study presents an extensive literature review about SWI with a focus on fractured crystalline-rock aquifer and an aquifer vulnerability assessment of Koster Islands specific to SWI. Using two modified multicriterion geographical information systems (GIS) based models (WELD-Ld and WELD-Mc), the vulnerability of Koster bedrock aquifers to SWI was assessed. Several parameters were used to capture the geomorphological and physical factors (e.g., fractures) which influence the flow of SWI in bedrock aquifers of Koster Islands. These spatially and semi-quantitatively methods are based on the well-known approach 'DRASTIC,' a systematic evaluation technique which incorporates major influencing factors. The WELD-Ld model uses five parameters (thematic layers) including Well density (W), Elevation (E), Lineament length (L), Distance to the sea (D) and Lineaments density (Ld) and WELD-Mc model uses map-counting (Mc) instead of Lineament density (Ld) calculation. The Mc analysis examines the inhomogeneity of Koster lineament distribution patterns. The impact (rate value) and significance (weight value) of each parameter in the vulnerability assessment was assigned based on previous studies and communication with experts. Lineament density (Ld) is the major influential factor in the vulnerability of the study area, which is related to the highly sheared and densely distributed Koster dyke swarm.

The overall vulnerability assessment maps show that the north and northeast part of the islands have a higher risk of SWI. The obtained maps have been compared with observation data from the study area and used to validate the models and identified areas and wells that may be at higher risk of SWI. In conclusion, the acquired results (vulnerability maps) incorporated with field studies can be a useful tool for decision-making and groundwater management.

Keywords: *Saltwater intrusion • Fractured bedrock aquifers • DRASTIC • Vulnerability mapping • Koster Islands*

Sammanfattning

Saltvattenintrång är ett av de stora hoten i många kustområden, främst drivet av antropogena processer (överpumpning) och klimatförändringar (havsnivåökning). Det har utförts omfattande forskning och teknikutveckling för att förstå och minimera SWI. Kvantifiering av och mekanismen för SWI förblir emellertid oklar och ofullständig, särskilt i uppsprucken kristallin berggrund.

Denna studie presenterar en omfattande litteraturöversikt över SWI, med fokus på en akvifer i uppsprucken kristallin berggrund och en sårbarhetsanalys över Kosteröarnas akviferer i relation till SWI. Genom att använda två modifierade multikriteriemetoder (WELD-Ld och WELD-Mc) med geografiska informationssystem (GIS) var det möjligt att bedöma sårbarheten för SWI hos Kosters berggrund. Flera parametrar användes för att spegla de geomorfologiska och fysiska faktorerna (t.ex. sprickor) som påverkar SWI i berggrundens akviferer. Dessa rumsliga och semi-kvantitativa metoder är baserade på den välkända metoden 'DRASTIC', en systematisk utvärderingsteknik som inkluderar stora påverkande faktorer. WELD-Ld-metodiken använder fem parametrar (tematiska lager) inklusive brunndensitet (W), höjd (E), lineamentlängd (L), avstånd till havet (D) och lineamentdensitet (Ld) och WELD-Mc använder "map-counting" (Mc) istället för lineamentdensitet (Ld). Mc-analysen undersöker inhomogeniteten i lineamentfördelningsmönstret för Koster. Effekten (kursvärde) och betydelsen (viktvärdet) för varje parameter i sårbarhetsbedömningen tilldelades baserat på tidigare studier och kommunikation med experter. Lineamentdensitet (Ld) är den viktigaste påverkande faktorn i sårbarhetsanalysen i studieområdet, vilken är relaterad till den starkt skjuvade och tätt fördelade intrusionsgångar förekommande på Koster.

De resulterande kartorna över sårbarhetsbedömningen visar att den norra och nordöstra delen av öarna har en högre risk för SWI. Kartorna har jämförts med observationsdata från studieområdet och identifierade områden och brunnar som kan ha högre risk för SWI. Sammanfattningsvis kan de genererade sårbarhetskartorna tillsammans med fältstudier vara ett användbart verktyg för beslutsfattande och hantering av grundvattenresurser.

Nyckelord: *Saltvattenintrång • Akvifer i uppsprucken berggrund • DRASTIC • Sårbarhetskartläggning • Kosteröarna*

Acknowledgments

This thesis has been produced during my scholarship period at the University of Gothenburg, funded by the Swedish Institute.

I want to thank all those who have supported me in different ways with my studies throughout the years: family, friends, and colleagues. I sincerely thank my supervisors, Dr. Markus Giese, for his consistent and valuable support during the thesis work. Thanks are also due to my examiner, Prof. Roland Barthel. Special thanks to Dr. Mark Peternell for helping me in the analysis part and providing the necessary information. I would also like to acknowledge Thomas Eliasson from the Geological Survey of Sweden (SGU) for his support and constative discussion.

Last, but not least heartfelt thanks to my family and my fellow students (Niclas Hultin, Mandana Farvardini, Henrik Engdahl, Axel Kilbo Pehrson, Axel Barkestedt and Andrea Håkansson) at Department of Earth sciences for creating an enthusiastic and stimulating working environment.

Contents

List of Figures

List of Tables

List of Abbreviations

DRASTIC	*Depth to the water table (D), Net recharge (R), Aquifer media (A), Soil media (S), Topography (T), Impact of the vadose zone media (I), and Conductivity (hydraulic) of the aquifer (C)*
EC	*Electrical conductivity*
EM	*Electromagnetic*
FDEM	*Frequency Domain Electromagnetic*
FFEC	*Flowing Fluid Electrical Conductivity*
GIS	*Geographic Information System*
GVC	*Geovetarcentrum, Gothenburg University*
IPCC	*Intergovernmental Panel on Climate Change*
IVL	*Swedish Water and Air Pollution Institution*
LiDAR	*Light Detection and Ranging*
Mc	*Map-counting*
R	*Rate value*
SGU	*Geological Survey of Sweden*
SLR	*Sea Level Rise*
SMHI	*Swedish Metrological and Hydrological Institute*
SNRA	*Swedish National Road Administration*
SWI	*Saltwater Intrusion or Seawater Intrusion*
SWICA-2 M3	*Salt Water Intrusion in Coastal Aquifers – Monitoring, Modeling, and Management*
SWIMs	*Salt Water Intrusion Meetings*
TDEM	*Time-Domain Electromagnetics*
V	*Vulnerability index*
W	*Weight value*
WELD-Ld	*Well density (W), Elevation (E), Lineament length (L), Distance to the sea (D), and Lineament density (Ld)*
WELD-Mc	*Well density (W), Elevation (E), Lineament length (L), Distance to the sea (D), and Map-counting (Mc)*

1. Introduction

1.1. Background

A sustainable supply of potable water is the most crucial and prominent resource for domestic usage, ecosystems, industrial, and agricultural activities (Naiman et al., 1995). A large proportion of the world's population depends on groundwater resources. Thus, these resources play a crucial role in providing a substantial amount of freshwater (Small and Nicholls, 2003). Nevertheless, in many coastal areas, freshwater aquifers have been exposed to SWI mainly due to disruption of natural hydrological conditions and climate change (e.g., FitzGerald et al., 2008; Post, 2005). Thus, it is essential to understand and manage this valuable and scarce groundwater resources to effectively plan and adapt to future changes, which requires detailed knowledge and information, such as hydrogeological properties and spatial variability (Bear et al., 1999).

On a global scale, SWI incidents are increasing. Sustainable groundwater resources management is still one of the main ongoing challenges for water resources managers and hydrogeologists. For more than a half-century, researchers from multiple disciplines have been working on understanding the dynamics of water flow in coastal and island aquifers. Nevertheless, processes underlying SWI are complex and challenging to define, both on a regional and a local scale (Post, 2005). SWI in crystalline bedrock is highly complex, mainly due to the highly heterogeneous and anisotropic nature of fracture systems (e.g., Neuman, 2005).

In Sweden, around 60% of drinking water supply is dependent on groundwater resources, making it a valuable natural resources (Kløve et al., 2017). The coastal areas and archipelago around Stockholm's (Boman and Hanson, 2004; Lindberg et al., 1996) and the Koster Islands (Banzhaf et al., 2017) have evident problems with SWI. The causes of SWI are mainly related to increasing exploitation of freshwater and decrease of precipitation (recharge amount). Typically, the cause of SWI is related to excessive groundwater extraction, which higher than the volume-rate that is recharged (e.g., Aronsson, 2013; Lång et al., 2006; Thunqvist, 2011). However, SWI in Sweden have been considered as a single (private) well problem and has not received much attention from environmental management and policymakers (Barthel et al., 2017; Boman and Hanson, 2004; Boman, 2004).

Water resources on the Koster Islands are mainly dependent on private wells situated in crystalline bedrock aquifers and unconsolidated sediment aquifers. Fractured bedrock aquifers on the islands are highly sensitive to overexploitation, while unconsolidated sediment aquifers are more vulnerable to contamination and drought (Barthel et al., 2016). Surveys conducted by Strömstads municipality have shown that SWI is more pronounced in drilled wells (wells in fractured bedrock aquifers), particularly in North Koster (Strömstads municipality, 2009). As a result, to avoid further contamination by saline water, drilling of new wells has been prohibited. Therefore, close evaluation and understanding of the hydrogeological system of Koster Islands aquifers are an essential step for stable use of freshwater resources and future planning.

1.2. Saltwater intrusion

Saltwater intrusion (SWI) is a surface and underground flow which contaminate freshwater resources, particularly in coastal areas and islands (e.g., Bear, 1979). The causes of SWI can either be the result of an anthropogenic or natural process or both (e.g., Werner and Simmons, 2009). Generally, there are three common mechanisms of SWI (Figure 1, e.g., Barlow and Reichard, 2010; Klassen and Allen, 2017):- 1) lateral intrusion of saline water due to the landward shift of the transition zone, 2) ascending of highly saline water from deeper parts of the groundwater system due to groundwater extraction (upconing), and 3) downward encroachment from coastal water due to inundation or storm surge. Depending on the effects and dynamics of the water density, SWI can occur at different scales ranging from meters to kilometers (e.g., Barlow, 2003).

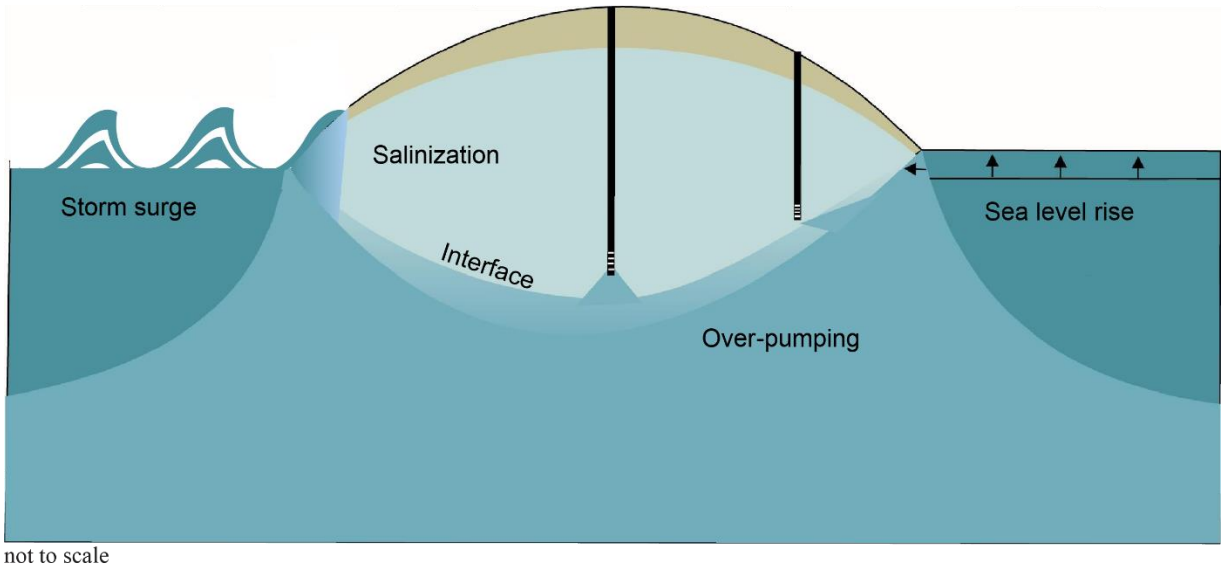

Figure 1 Schematic shows main causes of SWI (salinization of wells) due to sea level rise, storm surge, and over-extraction of groundwater. Light blue color represents freshwater lens (Klassen and Allen, 2017)

The interaction between saltwater and freshwater forms indistinct boundary mainly due to density difference (e.g., Abarca et al., 2007). Numerous studies use various terms in describing the mixing boundary between freshwater and saltwater, e.g., zone of dispersion, zone of diffusion, zone of mixing. In simplified conceptual models, the freshwater-saltwater interface term is used to represent the transition zone between freshwater and saltwater (Figure 1). Investigating and characterizing the freshwater-saltwater interface is a significant concern for effective groundwater management (Barlow, 2003). Cooper (1964) studied the relationship between freshwater and saltwater in a coastal aquifer. He concluded that density difference mainly controls the dynamics of the freshwater and saltwater interface. Studies conducted by Sund and Bergman (1981) found that high hydrostatic pressure of the freshwater leads groundwater to typically flow towards the sea, i.e., the hydraulic gradient slopes towards the sea. Under idealized conditions, freshwater flows seaward mainly due to density difference and forms a circular flow path in the mixing zone (Reilly and Goodman, 1985). However, other mechanisms, such as hydrodynamic dispersion and pressure gradients, are also related to the groundwater flow. The mixing zone is always in a transient condition continually changing in position and thickness, i.e., disturbance of the fragile balance between the freshwater and seawater due to various driving forces (Kim et al., 2009). For example, sea level rise or storm surge ease more seawater penetration, and the interface moves inland. By contrast, during

flooding the interface is pushed back to the sea by seaward-flowing freshwater, resulting seaward advance of the wedge.

1.3. Classification of SWI

Fetter (1973) reported two types of SWI: passive and active. Passive SWI refers to when fresh groundwater flows towards the sea against density-induced forces, i.e., hydraulic gradient slopes toward the sea. Whereas active SWI refers to the same direction (landward) flow of saline water and fresh water, i.e., hydraulic gradient slopes towards the land (e.g., Badaruddin et al., 2017). For further detailed description and discussion of these processes see, e.g., Badaruddin et al., 2017; Mahesha, 1995; Werner et al., 2013; Werner et al., 2012. The significant aspect of this classification is that it is crucial for understanding behavior of SWI dynamics in response to temporal and spatial changes, e.g., sea level rise (SLR) and pumping (e.g., Chang et al., 2011). However, most studies of SWI have mainly focused on passive SWI even though active SWI is evident in many areas (e.g., Fetter, 2001; Morgan and Werner, 2015; Yakirevich et al., 1998). The most common shift from passive to active SWI is caused by the decline of freshwater head, which increases salinity in aquifers (Allen et al., 2002; Badaruddin et al., 2015).

Recently, there has been renewed interest in investigating the behavior and effects of freshwater-saltwater interaction during active SWI (e.g., Badaruddin et al., 2017; Werner, 2017). However, most studies, have failed to take account of fundamental driving factors of active SWI such as buoyancy, dispersive, and adventive forces. To date, active SWI is incompletely understood in defining all influencing factors of the hydraulic gradient slope and its relation to timescale (Badaruddin et al., 2017). Also, a third type of freshwater flow situation was proposed by Werner (2017), which represents a combination of active and passive SWI with both landward and seaward flow simultaneously.

1.4. Major drivers of SWI

Several factors can cause or influence SWI in an aquifer such as climate change, pumping conditions, hydrogeological, and physiographic setting (Custodio and Bruggeman, 1987; Werner et al., 2013). In other words, SWI is the result of or linked to many processes and factors (e.g., SLR, aquifer thickness, and recharge fluctuation) which creates difficulties in identifying

the primary controlling factors (Figure 2, Essik, 2001). Impacts of anthropogenic interventions and the global phenomena of climate change are the major drivers and pose significant and rapid impacts on global water resources, particularly in small islands, (e.g., Holding and Allen, 2016; Werner et al., 2013).

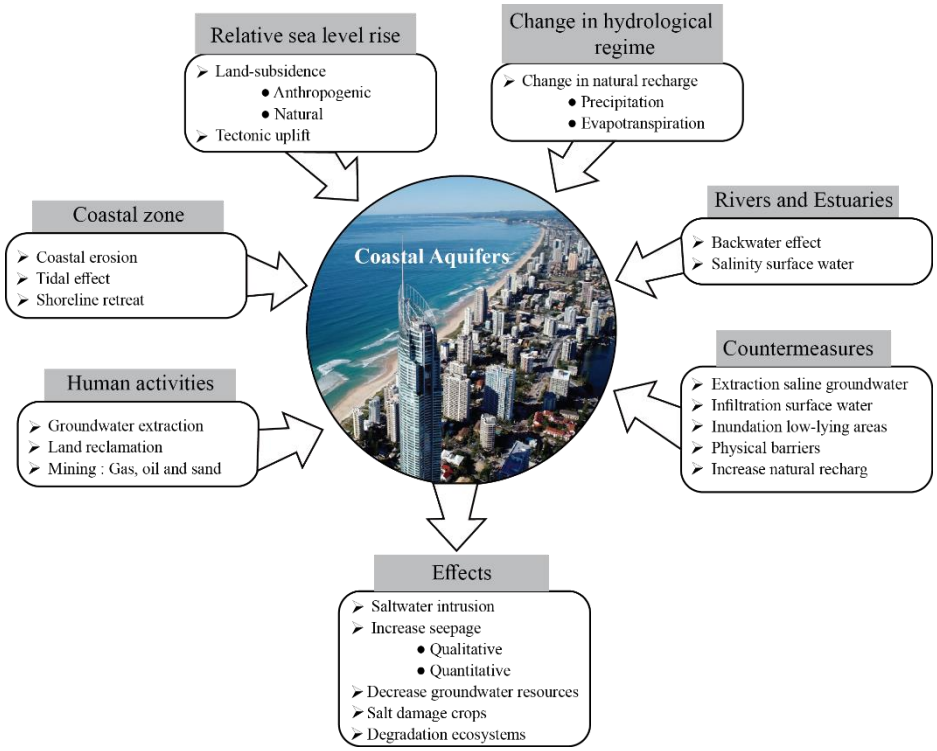

Figure 2 Major processes that are known to affect coastal aquifers, modified after Essink (2001)

1.4.1. Anthropogenic

Hazard threats from human influences and activities can significantly aggravate salinization risk such as over-abstraction of groundwater, and deterioration of recharge areas. Similarly, point source and nonpoint source pollution lower groundwater quality and alter groundwater chemistry such as oil refineries and sediment erosion, respectively (e.g., Allen, 2004; Han et al., 2015; Kanagaraj et al., 2018). Nevertheless, the impact of SWI has a more significant extent along the coastline (large-scale) in comparison to other subsurface pollutants. Thus far, intensive groundwater extraction due to increasing demands of water supplies and urban expansion has resulted in SWI and deterioration of groundwater and soil qualities in many regions of the world (Park et al., 2012).

A growing percentage of the world's population and a larger part of the world's population living in coastal regions adds immense pressure on groundwater reservoirs (Olofsson, 2005; Webb and Howard, 2011). Many parts of the world coastal regions are subjected to SWI especially densely populated areas (e.g., Netherlands) and arid and semi-arid regions greatly suffer from salinity and limited groundwater supply, e.g., India (Olofsson, 2005; Webb and Howard, 2011). Ferguson and Gleeson (2012) compared the vulnerability of coastal aquifers to groundwater extraction and climate change and showed that coastal aquifers are more vulnerable to overexploitation than climate change (e.g., sea level rise).

1.4.2. Climate change

Climate change such as SLR and precipitation fluctuations significantly impact groundwater characteristics in several ways, such as disturbance of the fragile natural equilibrium between freshwater and saltwater (e.g., Bobba, 2002; Lyles, 2000). The continued increase in the thermal expansion of oceans due to global warming has been significantly affecting the volume, and water quality of global water, which promotes SWI (Werner and Simmons, 2009). The warming of the earth causes changes in atmospheric pressure, increase water volume, facilitates the melting of glaciers and icecaps, which is major driver of SLR (Allen et al., 2014). To date, the Intergovernmental Panel on Climate Change (IPCC report) concluded with *high confidence* that there will be a continuous increase in global mean sea level, therefore a high risk of more saline water intrusion and inundation in coastal areas (Masson-Delmotte et al., 2018).

Similarly, seasonal precipitation changes (precipitation patterns) influence chemical and physical characteristics freshwater sources as well as groundwater flow pattern (Allen, 2004). For example, the decline in precipitation due to climate shifts can result in low recharge, which can ease SWI (Holding and Allen, 2015). Also, Werner and Lockington (2004) identified that salinization is more pronounced and higher during high tidal conditions.

On a global scale, the most recent, in geological timescale, major climate shift was during the glacial-interglacial cycles, which resulted in a significant change in the sea levels and caused large fluctuation in the saltwater and freshwater interface position. Following the glaciation, several regions were subjected to isostatic depression and caused submerged condition below sea level. During the Holocene and to date, the isostatic glacial rebound is still active at a

continental scale and highly pronounced in the coastal areas (e.g., Allen, 2004; Follin and Stigsson, 2014).

1.5. Fractured crystalline-rock aquifer

The term *fractured rock* is generally understood as a solid material which is intercepted with random generic discontinuities that occurred in response to stress. All rocks in the earth crust are subjected to stress and fractured to some degree. Stresses in the subsurface rocks are mainly determined and controlled by overlaying rock pressure and regional tectonic stresses (Banks et al., 1996). Each fracture has a unique characteristic with different flow properties, mechanical effects, and geometries. In fractured bedrock aquifers, a heterogeneous nature and limited primary porosity of the crystalline rocks create the main barrier in characterizing the configuration of the saltwater wedge and pathways of fluid flow. The heterogeneity and anisotropic nature of an aquifer form a non-uniform SWI and vary at a microscopic scale. Thus, a thorough analysis of tectonic structures of a rock formation is essential to understand the mechanism of groundwater in crystalline bedrock aquifers (Sund and Bergman, 1981).

In fractured crystalline bedrock aquifer, the flow of groundwater is dependent on the distinct nature of each fracture and its conductivity and porosity of the rock (Figure 3; Llopis-Albert and Capilla, 2010). Changes in groundwater level in fractured aquifers are affected locally whereas aquifers in unconsolidated sediments extend large scale. Moreover, groundwater in fractured crystalline rocks is dependent on the fractures transmissivity; and the transmissivity of a parallel plate opening of a fracture is directly proportional to the cube of fracture aperture (Snow, 1969). Also, Lång et al. (2006) reported that the contribution of a fracture to the permeability of a whole rock depends on its connection to other conductive fractures or fracture network. In other words, the fluid flow and yield of water in fractured crystalline-rock aquifer is dependent on the interconnection of fractures. Banks et al. (1996) identified three stress fields based on fractures. These are: (a) palaeostress fields which form initial fractures (i.e., water conduits) during rock formation (b) current in-situ stress which alters existing fracture geometry (c) artificial stress linked to abnormal external stress, e.g., human-made explosions. They also point out that fractures affected by in-situ stress plays a significant role in the dynamics of fluid flow. Also, Sund and Bergman (1981) concluded that rocks or formations exposed to in-situ

stress provide suitable reservoirs and conduits for groundwater compared to original fissures formed during rock formation.

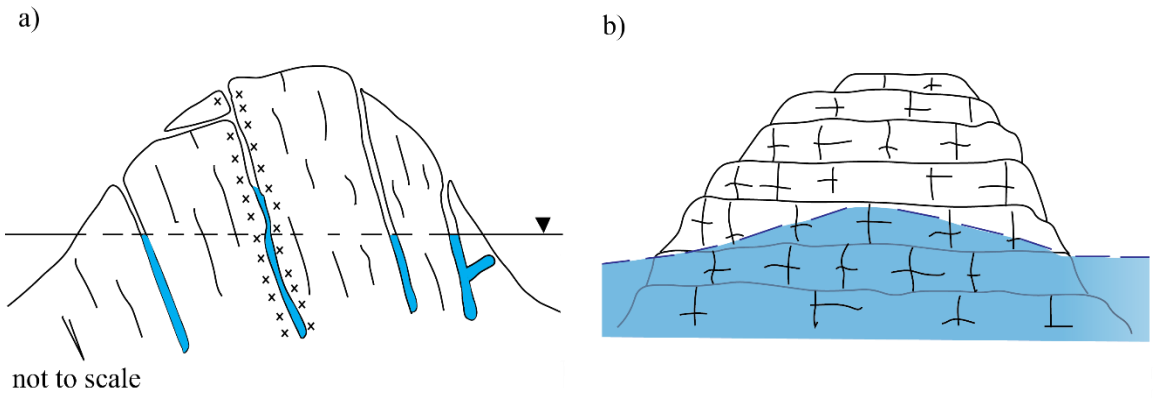

Figure 3 Simplified illustration of distribution of groundwater in a crystalline-rock aquifer (a) Gneiss - single fracture water level marked with (x), (b) Groundwater distribution in Granite, modified after Sund and Bergman (1981)

In the context of SWI, some well-documented studies reported that aquifer heterogeneities largely control or determine the thickness of transition zone and extent of SWI (e.g., Hodgkinson et al., 2007; Oki et al., 1998). Even though generalizing the characterization of aquifer heterogeneity is difficult researchers concluded that highly fractured and hydraulically conductive aquifer zones significantly facilitate the intrusion of saline water or discharge of fresh groundwater (Allen et al., 2003). However, transport properties in fractured aquifers remain unclear and poorly understood (e.g., Earon et al., 2015; Neuman, 2005).

Researches have been using field studies, laboratory techniques, and modeling to analyze SWI in fractured crystalline-rock aquifers. The majority of bedrock aquifer studies have been mainly focused on characterizing density and orientation of fracture networks to calculate the hydraulic conductivity and determine groundwater flow pathways (Llopis-Albert and Capilla, 2010). Moreover, they found that orientation of fractures significantly influences the flow of water in fractured aquifer. Comparatively, fractures aligned parallel to the hydraulic gradient have higher conductivity than fractures aligned perpendicular to the hydraulic gradient. Furthermore, studies by Gentry and Burbey (2004) generalized that well-connected lineaments and fractures network provide a better pathway for fluid flow in fractured bedrock aquifers, and thus is highly sensitive to water salinity during SWI. Also, soil layers and pockets of soil within fractured

rock system can act as essential water reservoirs as well as an entry point or exit points in the process of SWI (Earon et al., 2015; Freeze and Cherry, 1979).

1.6. Purpose and scope

The purpose of this research is to investigate the current state of knowledge of SWI, mainly in a fractured crystalline-rock aquifer and assess risks of SWI in Koster Islands. Contemporary challenges of limited understanding of the hydrogeological nature of fractured bedrock aquifers can be improved by integrating different approaches and identifying competent methods for effective groundwater management. Hence, this study attempts to use systematic multi-criteria hydrogeological GIS-based evaluation to examine the vulnerability of the Koster Islands aquifers to SWI.

This study is based on the following research questions:

1. What is the mechanism and process behind SWI and the driving force and causes of salinity problems in coastal aquifers?
2. What is the state of knowledge of SWI in coastal areas dominated by crystalline bedrock such as Sweden, Scandinavia, and countries with similar geology and climate?
3. What are the challenging questions and uncertainty of the SWI in fractured crystalline-rock aquifer?
4. Which methods exist to investigate, analysis, and describe SWI under conditions mentioned in questions 2?
5. What are the requirements for applying selected methods successfully, and what are the limits of such an approach?
6. What is the risk of SWI in fractured bedrock aquifers of Koster Islands?

1.7. Thesis outline

The scope of this study includes not only SWI vulnerability assessment of the groundwater aquifer in Koster Islands but also provides a brief review of the characteristics of the interface between freshwater and saline water and various approaches and tools used for investigating SWI mainly in fractured crystalline-rock aquifers. This report began with the overview and previous studies of SWI and followed by an exemplary case study on the Koster Islands.

2. An overview of SWI research

SWI effects have been a growing concern in the environmental management and have drawn attention in the research community with increasing number of studies and detailed analysis of coastal and island aquifers (Ghyben, 1888; Herzberg, 1901; Huyakorn et al., 1987; Pinder and Cooper Jr, 1970; Voss and Souza, 1987; Werner and Gallagher, 2006). Many studies have focused on improving the understanding of hydrogeological nature (e.g., groundwater supply) and in developing assessment techniques (e.g., groundwater modeling). Moreover, researchers have been working on developing assessment tools and providing in-depth information for policymakers and societies. Additionally, there are numerous regular scientific conferences where people share ideas, recommendations and review studies conducted in several locations for improving water security, effective groundwater management strategies, and long-term planning, e.g. SWIMs (Salt Water Intrusion Meetings) and Salt Water Intrusion in Coastal Aquifers – Monitoring, Modeling, and Management (SWICA-2 M3). However, the vast majority of SWI studies and assessment tools suffered from limitations due to their scale-dependent application and failed to integrate water security risks (Holding and Allen, 2016). Thus, the quantification of groundwater flow on a large scale is one of the ongoing challenges in the study of groundwater. In general, water flow in unconsolidated aquifers are well understood compared to fractured bedrock, which has limited well-developed assessments.

2.1. Worldwide studies

Around the globe, many SWI case studies have been performed using different approaches and tools. The majority of these studies were conducted in Europe, the Mediterranean region, and North America (e.g., Alcalá and Custodio, 2008; Custodio, 2010; Custodio and Bruggeman, 1987). Figure 4 shows the distribution of SWI case studies conducted around the globe, which are presented at Salt Water Intrusion Meetings (SWIMs).

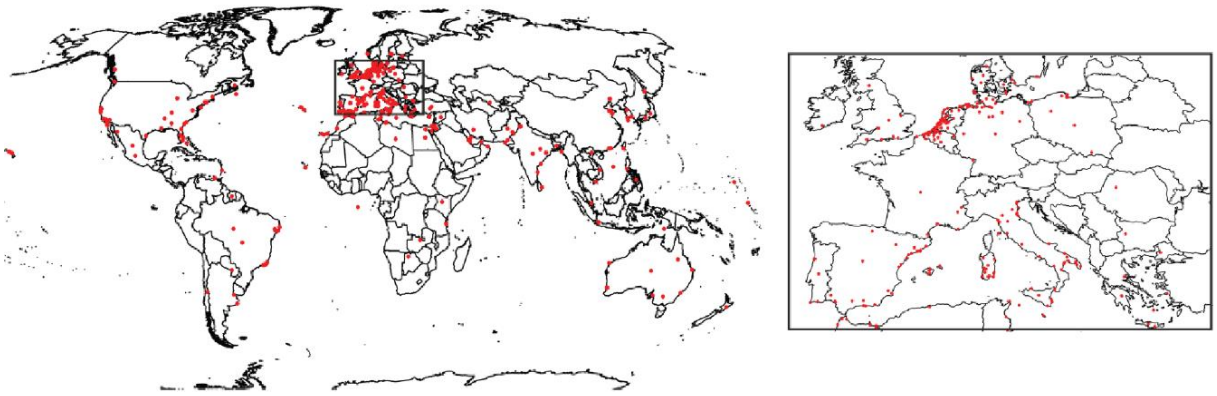

Figure 4 Locations of studies of saltwater intrusion (SWI) presented at SWIMs, and the inset map is an enlargement of Europe and the Mediterranean region, which have the highest density of SWI research (Post et al., 2018)

2.2. Sweden

Even though Sweden generally receives sufficient meteoric water and is rich in freshwater sources, SWI is evident in many areas, e.g., Stockholm archipelago (Olofsson, 2005). The Geological Survey of Sweden (SGU) has a long history conducting groundwater studies and archived detailed boreholes (well) data which have been drilled since 1979 and groundwater levels information starting from the end of the 1960s. In a study conducted by Lindewald (1981), approximately 80 wells (1%) of the wells drilled each year were reported as salt-water wells. Up to now, statistical information from SGU shows that around 3000 new wells are drilled each year in Sweden. Around the early 1980s, research and case studies began to emerge, which focus on SWI in Stockholm conducted by the Swedish Water and Air Pollution Institution (IVL). These studies adopted several approaches to investigating the extent and changes of SWI, particularly in southeast Vindö (Sund and Bergman, 1981).

Starting from the early 1970s, many countries including Sweden have been conducting a detailed investigation for locating a sustainable underground hard rock storage for high-level nuclear waste; e.g., Forsmark and Äspö (Black et al., 2017). As a result, there has been an increasing number of hydrogeological studies and groundwater modeling to understand the groundwater flow in crystalline rocks thoroughly (e.g., Hjerne and Nordqvist, 2014). The primary purpose and focus of these studies were safety assessments and site suitability for disposal of toxic or radioactive wastes in deep-lying crystalline rock. These studies also encompass the effect of saline water intrusion on the high-level nuclear waste repository and

have resulted in developing a model and approach in understanding the groundwater flow patterns (Vidstrand et al., 2014; Vidstrand et al., 2013).

Abandoned mine sites and tunnels have also been used as experiment sites for studying groundwater flow in fractured crystalline rocks (e.g., Stripa Mine) and its hydrogeological changes after mining and material excavation (Black et al., 2017). Additionally, SGU has been conducting regular hydrogeological mapping and developed maps which show areas with a high probability of encountering saltwater after drilling. Nevertheless, little is known and has been done on the assessment of SWI in Sweden.

2.2.1. Sources of saline water

In Sweden, saline water contamination is related to three sources: intruded saline water, relict seawater, and anthropogenic salinization. Relict seawater intrusion and anthropogenic salinization are related to saline water contamination derived from the marine environment (fossil water) and surface pollutants, respectively. However, it is not straightforward to identify this classification. Identifying sources of saline water can be valuable information for water and environmental management, particularly in finding a remedy and proper monitoring for SWI.

1) Intruded saline water

In many coastal areas of Sweden, the dominant presence of saline water in the wells is mainly related to SWI. However, there are no detail studies on differentiating between saline water derived from intrusion or fossil saline water (Nordberg, 1981). The glacial advance, glacial maximum, and glacial retreat are the extreme climatic conditions which have significantly influenced the hydrological setting of the Fennoscandian shield.

2) Relict seawater

Several studies in Sweden have discovered the existence of unflushed relict seawater in sediments pockets within the bedrock aquifers (Nordberg, 1981) and interpreted it depending on the geology, hydrogeological environment, and depth of groundwater. Even though tracing fossil water is complicated, some case studies conclude that the origin of deep saline water in an aquifer is related to the paleo-marine environment, i.e., during and after the latest deglaciation. In geological periods fossil water is believed to be trapped during the late

Wisconsinan glaciation (Gewers and Håkansson, 1988; Lundqvist, 1986). Mainly the geographical location and elevation of contaminated wells were used to identify the origin of saline water, referring to the Holocene marine level (Lindewald, 1981). The chemical composition of fossil water acquired from the crystalline basement, Paleozoic sedimentary rocks and unconsolidated deposits highly match with the extent and distribution map of the postglacial sea.

3) Anthropogenic sources

Saline pollutants such as road salt and leaky chemical storage are major sources that may contribute to the salinity of groundwater resources. In Sweden, during winter periods, the influence of road salt usually increases salinity content of surface water and groundwater. Statistically, since the 1970s, there has been a rise in chloride concentration in freshwater resources in response to the increasing amount of deicing salt (Thunqvist, 2011). A study conducted in the river basin of Sagån concluded that more than 50% of the total chloride load in the river was derived from the road salt applied by the Swedish National Road Administration (SNRA).

2.3. Methods used to investigate SWI

Different approaches and techniques with varying degree of complexity have been developed to understand both the interaction between saltwater-freshwater and causes of SWI. Even though there has been an increasing advancement and invention of powerful equipment, the forecast and monitoring SWI remains elusive, particularly in fractured crystalline-rock aquifers (Sanford and Pope, 2010). Scarcity of input data has also been a problem in determining the behavior of the transition zone, e.g., modeling (Olofsson, 2005).

Nevertheless, the characterization of transient and highly heterogeneous aquifers in a complex environment can be improved by using multiple methods (i.e., integral approach) at a single site, e.g., (Allen et al., 2003; Dogan et al., 2014). In general, any technique or groundwater model is defined based on their range of applicability (scale) and ability to integrating different criteria (e.g., isotropic, homogeneous). The following sections present an overview of standard non-modeling methods and analytical techniques used in a variety of landscape and

hydrogeological settings. Most of these methods were first employed for other purposes and later adopted for the studied of SWI.

2.3.1. Hydrochemical and isotopes analysis

Close examination of chemical properties of the water samples has been used to study the origin of the chemical constituents in groundwater and changes of groundwater chemistry. Previous studies used stable isotopes (e.g., hydrogen, oxygen, and bromide) and ion concentration analysis to determine the possible source (chemical evolution) of salinity in an aquifer. Also, used to develop a conceptual model of flow patterns in coastal and island aquifers (e.g., Allen, 2004; Bein and Arad, 1992; Jørgensen et al., 2008). Particularly isotopes analysis is found to be effective in areas which have been subjected to glaciation and postglacial isostatic. Furthermore, this approach is also used in analyzing the interaction between water and rock. The following are some of the common isotopes used in analyzing and identification of SWI.

Cl/Br ratio have been extensively used to identify salinity sources such as road salt, seawater, and deep basin brines (e.g., Katz et al., 2011). The conservative nature, i.e., resistant to water-rock interaction, and existence in all-natural water makes the Cl/Br ions preferable advantageous tracer. The Cl/Br ratio reflects the origin of chloride in groundwater even though changes in the absolute concentration is evident due to changing processes. Recharge from precipitation is also estimated using the amount of atmospheric chloride (unique characteristics) in groundwater. This type of method has been proven to be useful in enhancing the understanding of the groundwater system and in tracking groundwater contaminants (Alcalá and Custodio, 2008; Wilson and Long, 1993). Nevertheless, many studies have claimed that Cl/Br ratio is affected due to iron oxidation in soil and decay of organic matter which leads to sorb bromide (Davis et al., 2004; Vengosh and Pankratov, 1998).

Similarly, strontium isotopes are ($^{87}Sr/^{86}Sr$) is one of the frequently used isotopes for tracing the evolution of groundwater and seawater-freshwater mixing. Based on the strontium isotope ratio, studies have shown to identify the mixing system of the groundwater with various water types (e.g., Jørgensen et al., 2008; Langman and Ellis, 2010; Lara and Weber, 2010). Strontium isotope investigation with ion analysis and mixing analysis is used to create a conceptual view of a distribution of different water types and complex flow paths.

2.3.2. Geophysical and geological approach

Geophysical investigations unveiled more subsurface information such as detecting the occurrence and possible pathways for SWI, e.g., groundwater modeling (e.g., Siemon et al., 2009). Several studies have highlighted the critical competence of geophysical techniques in hydrogeological investigations, for locating the saline wedge (interface) and characterizing aquifer heterogeneity (e.g., Allen et al., 2002; Comte et al., 2017; Duque et al., 2008). Some advantages of these techniques are that it is cost-effective and easy to conduct compared to other methods, such as drilling (Himi et al., 2017). Also, geophysical methods, in combination with geological and hydrochemical data, can further enhance and increase the confidence in monitoring and modeling groundwater flow patterns.

Electrical conductivity. Electrical conductivity (EC) is used to indirectly measure the dissolved ions concentration in groundwater using downhole and surface survey (e.g., Doughty et al., 2017; Park et al., 2012). The natural chemistry of the saltwater and direct relation between conductivity and salinity acts as a natural tracer. In general, in a groundwater survey, a sudden change in the conductivity reflects or is related to the location of the saline wedge (Custodio and Bruggeman, 1987). Augmented SWI and flow of saline water towards the land along the coastline are linked to high EC values (Himi et al., 2017). However, this method of analysis has some limitations, such as difficulties in differentiating the cause of high conductivity that can also be attributed to, e.g., the properties of the basement or conductivity of clay minerals (Duque et al., 2008).

Electrical resistivity. Electrical resistivity has been extensively used for characterizing the hydrogeological environment and proven to be the most effective approach to estimating the depth of freshwater and saltwater interface (e.g., Nowroozi et al., 1999). Electrodes and geoelectrical probes, which are calibrated by lithological and hydrogeological information, are used to detect the resistivity contrast between freshwater and saltwater zones. There are numerous types of electrode configuration of which few of them are commonly applied. The information acquired from electrodes such as vertical resolution depends on the configuration (e.g., dipole-dipole configuration) and distance of electrode and probe (Poulsen et al., 2010). Studies reported by Dahlin and Zhou (2004) found that gradient configuration offers better signal-to-noise ratio with average effectiveness in most scenarios.

Electromagnetic. Initially, the electromagnetic (EM) application was invented for discovering ore bodies, mainly for base metals. However, numerous studies have shown that it is also convenient for mapping ground conductivity to study subsurface hydrogeological features (Stewart, 1982). This method measures the electric and magnetic fields of the underground materials and differentiates them depending on the electric conductivity. However, this approach requires lithology information to interpret it correctly in order to discriminate EM values generated from the geological formation, i.e., clayed sediment. Thus, without lithological information, the fixed resistivity threshold approach fails to accurately discrimination fresh from saline groundwater in the presence of clay sediments. There are the most common types of EM techniques:

1) Time-domain electromagnetic (TDEM) soundings measure the electrical property of subsurface, i.e., the electrical resistivity is found to be useful in identifying the distribution and extent of SWI. Saline water in aquifers are generally distinguished by low resistivity (e.g., Balia et al., 2003; Choudhury et al., 2001; Guérin et al., 2001). However, in some cases, the low resistivity zone could be due to the geological characteristics of the aquifer in such scenario, e.g., gravimetric method is applied to locate depth of an aquifer basement. A similar scenario is also typical in the electrical resistivity method.
2) Frequency Domain Electromagnetic (FDEM) method yield valuable information about groundwater dynamics and aquifers properties. Likewise, TDEM is used to investigate and map out SWI distribution in aquifers.
3) Airborne electromagnetic (Airborne EM) method cover large areas with significant penetration in a short time. It is a very competent, quick, and cost-effective tool for acquiring hydrogeological data and mapping groundwater system even in an inaccessible terrain (Delsman et al., 2018). To date, there are various systems of Airborne EM developed by different institutions and companies. Airborne EM technique found to be adequate for complex geological environments (e.g., fractured crystalline-rock aquifers) and yield excellent results when compared to ground-based measurements (e.g., Gilgallon and McGivern, 2018; Kirkegaard et al., 2011; Viezzoli et al., 2010). However, it is limited in spatial resolution when used on a local scale, which causes difficulties in identifying detailed complex flow system.

Gravimetry. Gravimetric tools are used to measure fractional changes of earth gravity filed (anomalies) created by the density difference of various material in the subsurface. The gravity

method has been widely used for delineating structural features and bedrock boundaries, which can provide crucial information about bedrock aquifers (e.g., Bohidar et al., 2001). Comparatively, gravity anomalies are least distracted by human-made material, such as water pipelines (Bohidar et al., 2001). However, due to some effects which masks or distort the earth gravity field this method requires accurate measurements and several corrections, such as latitude correction before using initial gravity values (raw data) (Blakely, 1996; Hinze, 1990).

Hydraulic tests. Hydraulic tests are also efficient and convenient in contributing valuable information for analyzing the dynamic behaviors of fresh-saline water interactions (Comte et al., 2017; Park et al., 2012). Hjerne and Nordqvist (2014), reported that there are two broad categories of hydraulic tests, which are: a) single borehole test, and b) hydraulic interference test. The main difference is that, in the case of hydraulic interference test, data is acquired from several boreholes measurement, while in single borehole tests, all data are collected from one borehole. In the SWI context, most of the hydraulic analysis is used for determining the transmissivity and hydraulic properties of an aquifer (Tsang et al., 2016). Slug test and pump test have also been extensively used in hydrogeological investigations and provide substantial support in estimating a hydraulic conductivity distribution of subsurface flow (Engard et al., 2005).

Boreholes. Boreholes logs are well known in providing subsurface lithological information and used in calibration (e.g., modeling) and correlating to results acquired by different methods. Besides, boreholes are effective opening for hydraulic and transport field experiments to understand the hydrogeology of the deep subsurface, e.g., Flowing Fluid Electrical Conductivity (FFEC) (Doughty et al., 2017; Tsang et al., 2016). Using FFEC approach, researchers have been able to define the hydraulic structure of crystalline rocks and investigate hydraulically conductive zones (e.g., Doughty et al., 2017). Perhaps the most demanding requirements and limitations of this method is that it is costly, provides limited spatial coverage (point information) as well as time-consuming depending on the geological characteristics of the subsurface and depth. Additionally, some methods conducted in a borehole are dependent on the depth of the well; for example, a conductivity survey is not possible in shallow boreholes (Duque et al., 2008).

FFEC logging approach had been helping hydrological studies to understand the subsurface groundwater flow geometry, which is conducted in a borehole during or after drilling. Using this approach, researchers have been able to identify hydraulically conductive fractures in a borehole (e.g., Moir et al., 2014; Tsang et al., 2016; West and Odling, 2007). This method is also advantageous because it can be conducted in a short period, e.g., during drilling breaks.

Another tool used in a borehole is an acoustic televiewer which is used to determine structural information, e.g., fracture orientation, by transmitting and receiving acoustic waves (Park et al., 2012). Difficulties arise, however, during differentiation of conductive and non-conductive fractures. Thus, to overcome this limitation, researchers used various types of flowmeter tests for identifying conductive fractures and determine their hydraulic conductivity (e.g., Le Borgne et al., 2006). By integrating field tests (e.g., acoustic logging) and monitoring data (e.g., EC), researchers have been able to characterize fractured rock aquifer and their variability with time and changing conditions (e.g., Park et al., 2012). Similarly, video and photo logging are acquired to deliver a realistic lithological, and structural information of the subsurface rocks and this information is used for model calibration and correlation (e.g., Allen et al., 2002).

2.3.3. Analytical approach

Ghyben – Herzberg method

Since the late 19th century some studies have established mathematical equations as a tool in predicting the position of the freshwater-seawater interface. In the late 1800s, Ghyben (1888) and Herzberg (1901) introduced one of the most frequently and widely used formula (Equation 1) for quantitatively estimating the depth to freshwater and saltwater interface for a steady-state and unconfined aquifer. The equation was developed based on the relationship between the freshwater zone that lies above (h) and below sea level (z) and density difference of freshwater and saltwater (Figure 5). The oversimplification is that the formula implicitly assumes only steady state condition, i.e., no vertical head gradient (Reilly and Goodman, 1985).

$$z = \frac{\rho_f}{(\rho_s - \rho_f)} h \qquad (1)$$

with *z* the thickness of the freshwater zone below sea level (m), ρ_f the density of freshwater (g/cm^3), ρ_s the density of saltwater (g/cm^3), and *h* the thickness of the freshwater zone above sea level (m) (Figure 5).

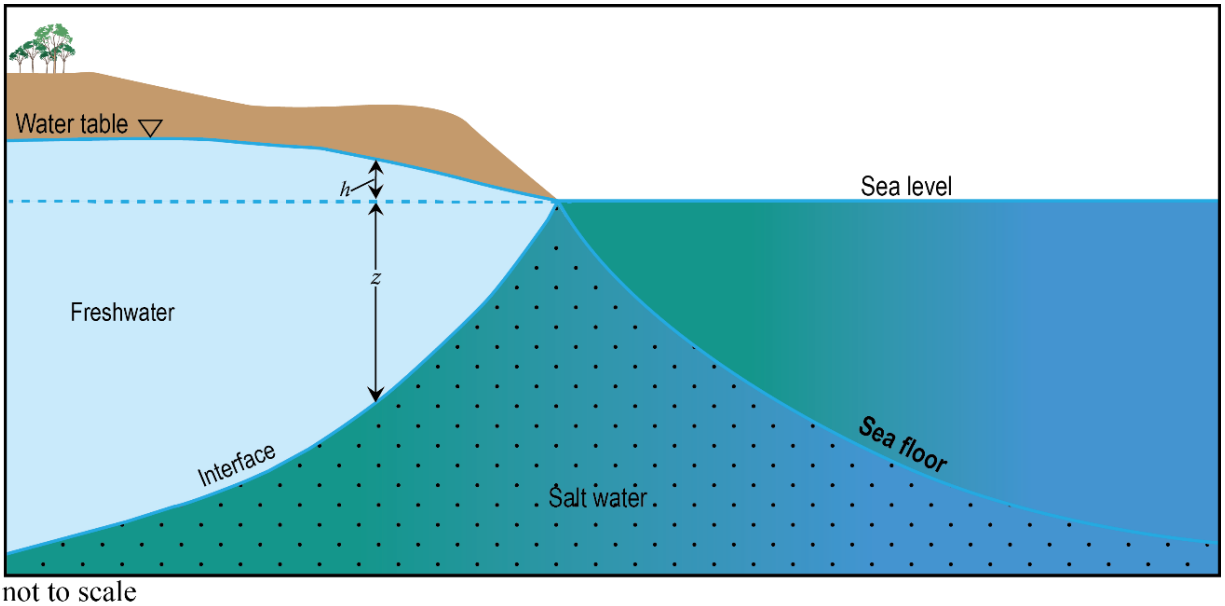

not to scale

Figure 5 Schematic showing interface position of an aquifer and the relationship between z (thickness of the freshwater zone below sea level) and h (the thickness of the freshwater zone above sea level) based on the Ghyben-Herzberg relation, modified after Barlow (2003)

Equation 2 shows a simplified version of equation 1, with freshwater density ρf = 1.000 g/cm^3 and saltwater density ρ_s 1.025 g/cm^3 at 20^0 C. According to Equation 2, a minor shift in the water, the table results in a significant change in the freshwater thickness. In other words, the 1-meter freshwater zone above the sea (*h*) corresponds to 40-meter fresh water below sea level (*z*).

$$z = 40h \qquad (2)$$

3. Koster Islands case study

The following chapter presents an overview description of the study area, including geological and hydrological setting as well as climate conditions.

3.1. Study area

3.1.1. Geographic setting

The study area (Figure 6) is located along the southwest coast of Sweden near the international border of Sweden and Norway (Latitude: 58.8958° N, Longitude: 11.0086° E), about 10 km west of Strömstad municipality. The study area (Koster Islands) comprises two major islands, North Koster (Nordkoster) and South Koster (Sydkoster). The North and South Koster Islands are the largest islands from the group of islands (Koster archipelago) with an aerial cover of 4km^2 and 8km^2, respectively. The Koster strait, an SW-NE trending rift valley, splits these islands into North and South Koster. The islands are separated from the mainland by ~ 250 meters deep and 3 km wide Kosterfjorden. The Kosterfjorden is known by its high level of salinity content, which is related to the North Atlantic deep-water flow and diverse marine species (Liljenström and Björk, 2013). The landscape of the Koster Islands is dominated by flat bedrock and hills, with the highest above sea level (58.8 meters) located in Kosterbonden, North Koster.

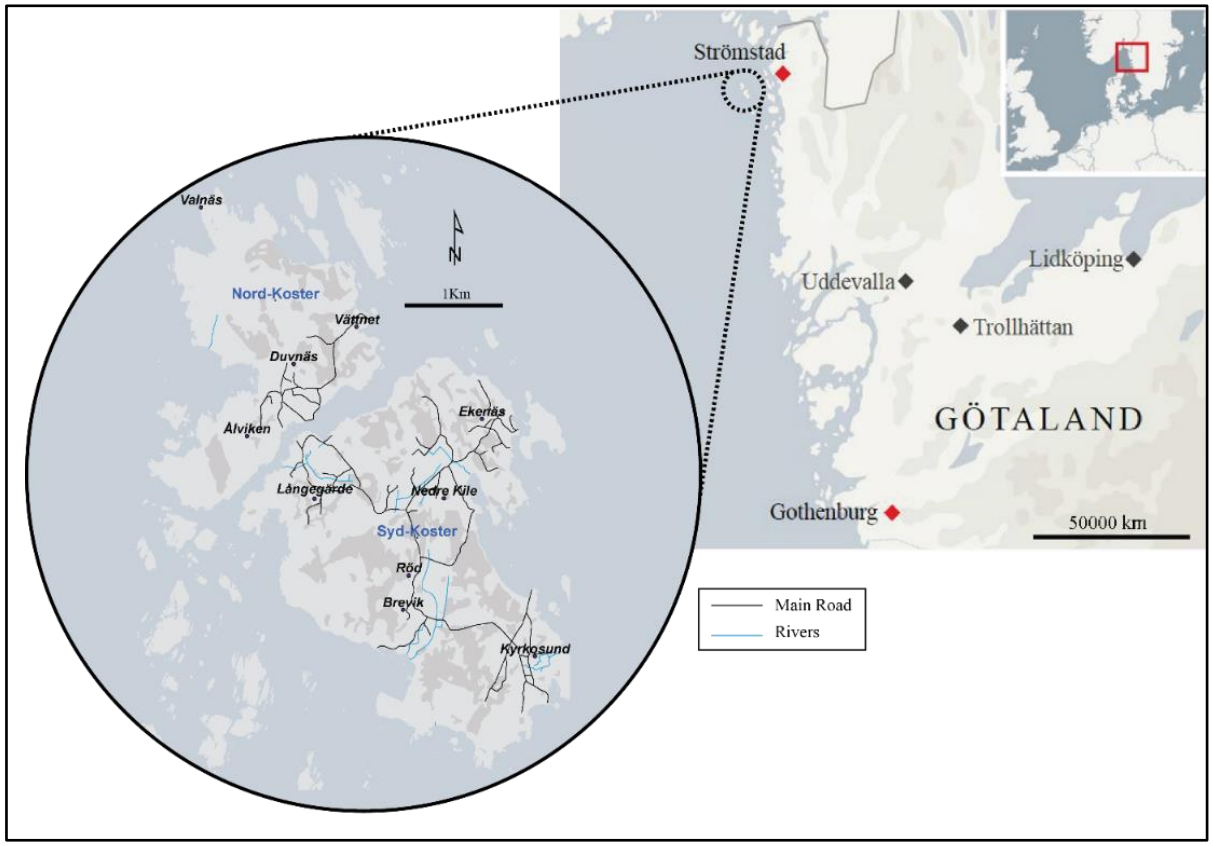

Figure 6 Location map of the Koster archipelago, modified after Nicholson (2014)

3.1.2. Geological setting

The geological formation of the Koster Islands is part of the Østfold-Marstrand belt (slab) which is mainly composed of granite and gneissic rocks. The genesis of the Koster Islands bedrock is divided into two main orogenic periods: Gothian (1700 - 1600 Myr B.P.) and Sveconorwegian (1200-900 Myr B.P.) (Hageskov, 1985). During 1600-1200 Myr B.P. (Kosterperioden) less pronounced orogeny occurred. Post the Gothian orogeny the Koster formation were dissected by numerous ca. 1420 Ma old dykes and sheets (e.g., Koster dyke swarm). The Koster archipelago geology has been divided into three major formations: Stora Le-Marstrand Group, Långegärde Tonalite, and Vettnet Granite (Nyström and Wall, 1993) (Figure 7). The Stora Le-Marstrand Group ages around 1560 Ma covers a large portion of Koster Islands and mainly composed of sedimentary gneiss rocks with layers of amphibole. The Långegärde Tonalite dominantly occur in the western part of the islands is dated to approximately 1560 Ma and composed of highly metamorphosed tonalite to granodiorite.

The geology of the Koster archipelago has been an interesting site in the investigating and understanding the geological history of the Sveconorwegian province of the Baltic shield. Notably, there has been an increasing amount of studies and interest on the Koster dyke swarm and pointed out as a remarkable spot in most of the Precambrian geology and evolution of the Baltic Shield (e.g., Lundqvist, 1979; Magnusson, 1963).

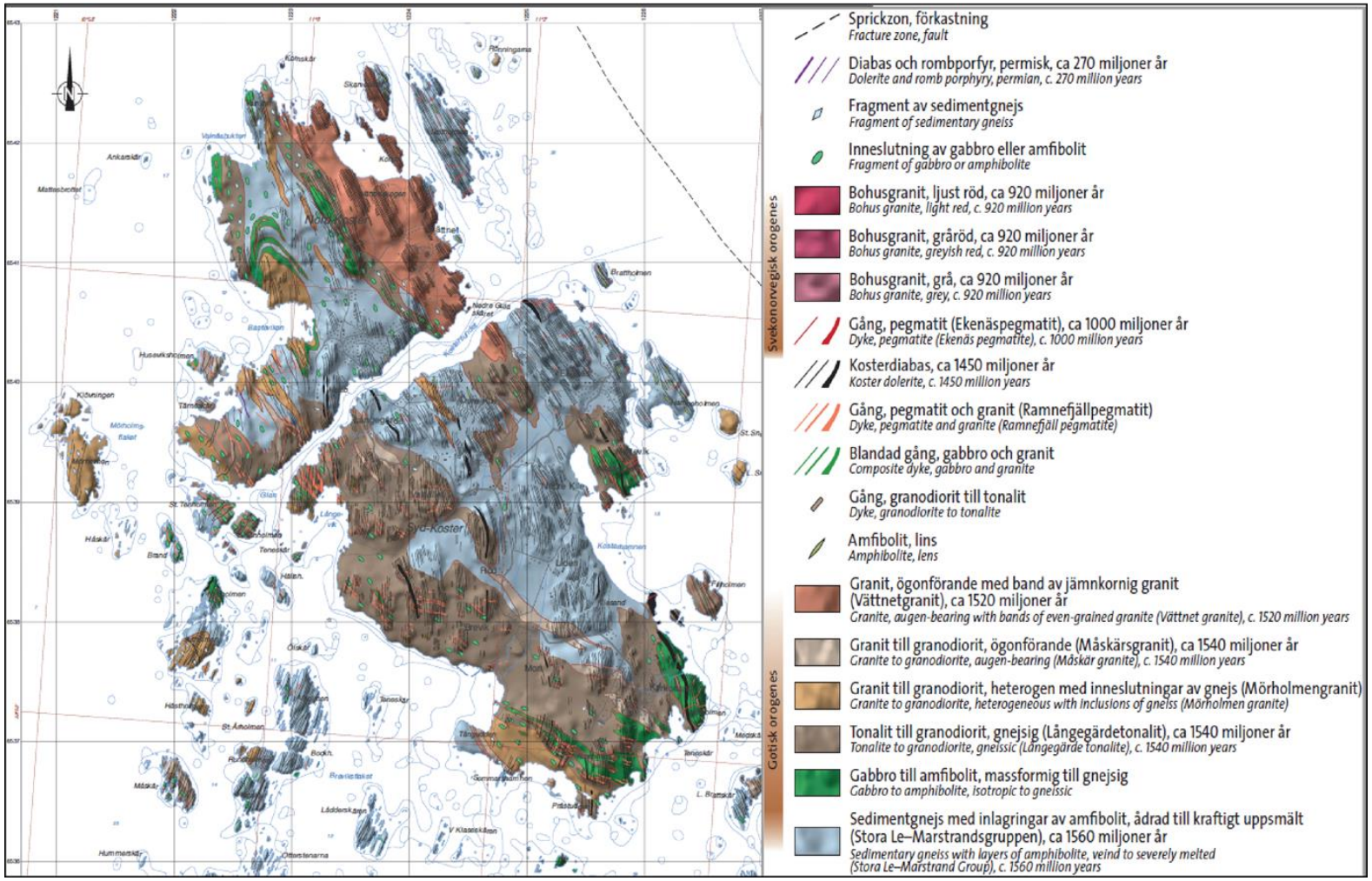

Figure 7Bedrock map of Koster archipelago (Eliasson, 2011)

3.1.3. Hydrogeological setting

In general, the regional hydrogeology setting of the Swedish coasts is mainly composed of bedrock, and unconsolidated sediments aquifers, where bedrock aquifers have limited storage capacity and water accumulation in unconsolidated sediments are scarce (SGU, 2019). Fractured bedrock aquifers dominate the Koster Islands with thin layers of unconsolidated sediments (Figure 8). The bedrock aquifers consist of predominantly granite and gneiss rocks with dominant NW-SE fractures and Koster dyke swarm (Figure 7). Fractures opening between the Koster diabase dykes and bedrock significantly influence groundwater flow or make up the fracture network, which mainly contributes to conductivity or storage of an aquifer (Nyström and Wall, 1993). Tectonic activity, i.e., dyke's intrusion, during the Sveconorwegian orogeny, has resulted in a network of nearly vertical fractures (Koster dyke swarm). Subsequently, an intense deformation and alteration of the dyke swarm contributed to the change of the primary fracture system (Hageskov, 1985). The porosity behavior of bedrock aquifers is often related to the fracture density and aperture of fractures (dyke opening).

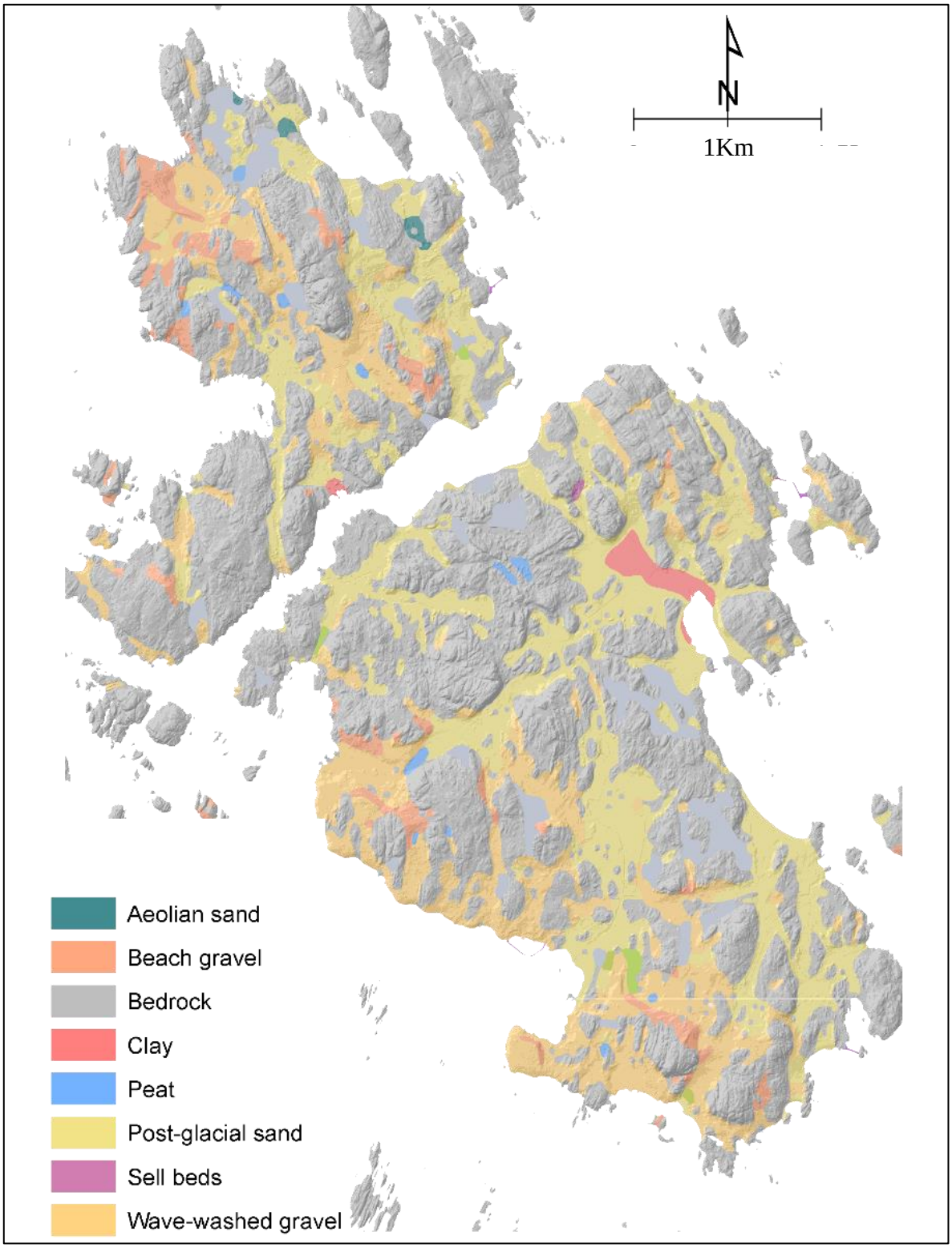

Figure 8 Unconsolidated sediment of Koster Islands

Around 300 permanent inhabitants of Koster Islands are dependent on private dug and drilled wells. In the islands, about 800 private wells extract water from thin layers of unconsolidated sediments and bedrock aquifers. However, freshwater resources are threatened by SWI,

especially during the summer period, when there is a peak in the number of visitors ranging from 6000-10000 (Banzhaf et al., 2017).

3.1.4. Climate

Temperature and precipitation data recorded by climate station situated in North Koster are available from the Swedish Meteorological and Hydrological Institute (SMHI). The Koster Islands lie within the humid continental climate and have mild, windy winters and warm sunny summers (Nyström and Wall, 1993). Monthly averages for precipitation and temperature are shown in Figure 9. The mean annual precipitation on Koster Islands is 714 mm/year (2005-2015) and 627 mm/year (1961-1990). The mean annual temperature ranges from 6.1°C to 12°C. In winter, the mean temperature falls to a minimum of −1.6°C while in summer it reaches a maximum of 20°C. Exceptional low precipitation periods, which lead to low groundwater levels were recorded during the years of 1976 -1977 and recently during the years of 2016 – 2017 (SGU, 2018). These dry periods have mainly affected the southern part of Sweden.

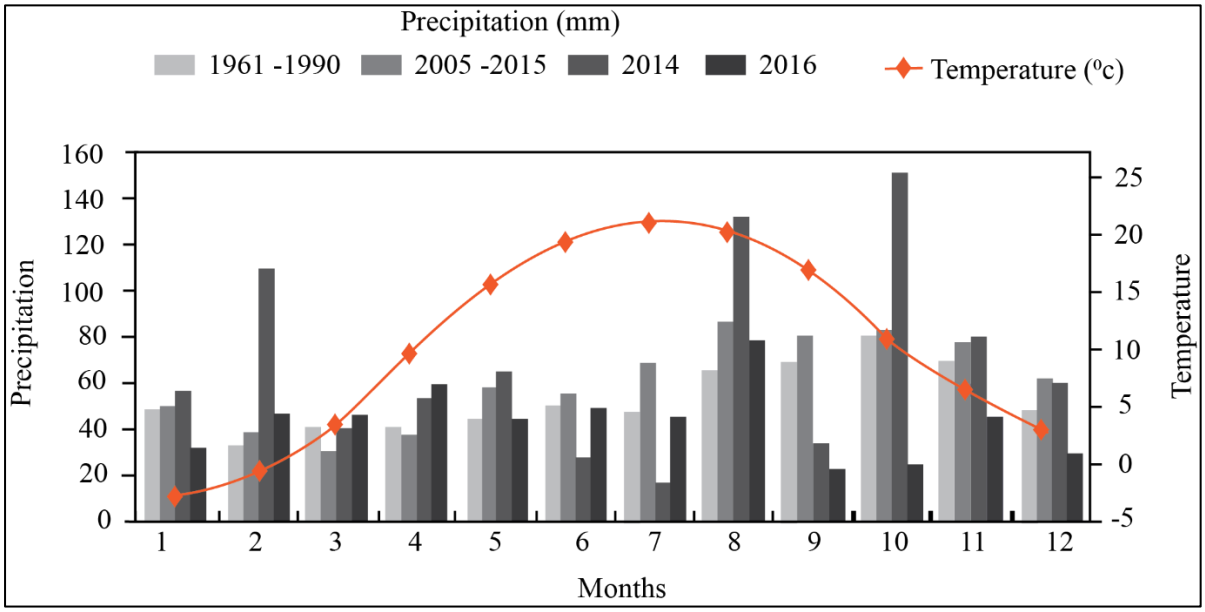

Figure 9 Shows mean annual precipitation and temperature (SMHI)

4. Materials and Methods

4.1. Data sources

The input data for the multi-criteria GIS-based analysis (vulnerability assessment) was derived from various data sources. The dataset used in this study are summarized in Table 1 and included overview maps (e.g., shoreline, lineaments, and lithology), topography layer, and spatial distribution of drilled well.

Table 1 Input and validation data used in the vulnerability assessment of the Koster Islands

Data Type	***Source***	***Format***	***Scale***	***Date***	***Used to produce***
Digital elevation model (DEM)	Lantmäteriet	Raster	2m	2010	E
Water Well	SGU	Point Shapefile	-	1976-2019	W
Bedrock & overview map	SGU	Polygon Shapefile	1:50 000 - 1:250 000	1960-2019	L, D, Ld, & Mc
Observation data	GVC	Tabular data	-	2016-2017	Comparison

SGU: Geological Survey of Sweden; GVC: Geovetarcentrum, Gothenburg University; W: Well density; E: Elevation; L: Lineament length; D: Distance to the sea; Ld: Lineament density; and Mc: Map-counting

4.2. Methods

The method applied in this study is based on one of the most popular groundwater vulnerability assessment method 'DRASTIC', developed by a committee of the US Environmental Protection Agency and the National Water Well Association (Aller, 1985). Also, a similar risk assessment conducted on the east coast islands of Sweden, i.e., Gotland (Ebert et al., 2016) and Öland (Eriksson et al., 2018). These risk assessments method is an index-based model, which have been widely applied throughout the world. Regional scale application, compatibility with GIS mapping and ease of use are some of the advantages of this method (e.g., Al-Adamat et al., 2003; Qian et al., 2012; Panagopoulos et al., 2006).

The risk assessment method, e.g., DRASTIC, describes the vulnerability of an area (assess groundwater contamination potential) based on influencing factors such as geologic and hydrogeologic setting. The initial letters of these seven parameters form the acronym "DRASTIC." This approach evaluates vulnerability index of groundwater based on the ratings and weights assigned to seven parameters, namely: Depth to the water table (D), Net recharge (R), Aquifer media (A), Soil media (S), Topography (T), Impact of the vadose zone media (I),

and Conductivity (hydraulic) of the aquifer (C). The rating and weights of each parameter are recommended to be modified in order to better reflect local conditions (Aller et al. 1987). The vulnerability index (*V*) is the result of a linear addition of weighted factor (*Wi)* and rating value (*Ri*) of the contributing factors calculated as:

$$V = \sum_{i=1}^{p} Wi \cdot Ri \qquad (3)$$

4.2.1. Development of the aquifer vulnerability maps

The model parameters used for the Koster Islands groundwater vulnerability mapping were selected based on the geologic and hydrogeologic setting. Also depending on the availability of reliable data required for calculating the vulnerability index, i.e., input data for each factor. The DRASTIC approach is limited in representing structural characteristics of fractured bedrock aquifers, such as fractures density (Aller et al. 1987; Wei 1998). As a result, the DRASTIC parameters were not used in this study, except topography. Based on the study area aquifer system (fractured bedrock aquifers) and similar previous assessment in other study areas with similar physical characteristics, modified vulnerability assessment models were developed.

In this study, six parameters were used to capture the hydrogeological system and create the final vulnerability maps: Well density (W), Elevation (E), Lineament length (L), Distance to the sea (D), Lineament density (Ld), and Map-counting (Mc) in order to adequately represent the influencing factors of Koster Islands aquifers. Using these model parameters, two modified models were developed: WELD-Ld and WELD-Mc. The ‘‘WELD-Ld’’ and ‘‘WELD-Mc’’ are the acronym for five model parameters, where the Lineament density (Ld) was replaced by Map-counting (Mc). The Map-counting (Mc) parameter shows the inhomogeneity of the Koster Islands lineaments, described in section 4.2.1(6)). Calculation of vulnerability index (*V*) involves these parameters, where each parameter is assigned a specific rating value (*R*) and weight value (*W*), as shown in Table 3. The significance of one factor over another and contribution of each factor to the overall susceptibility of an area are specified by the rating value (*R*) and the weight value (*W*), respectively (Aller et al. 1987). The weight and rating value ranges from 1 (very low) to 5 (very high). The rating value (*R*) was assigned after each

parameter were classified into five classes based on the influence and its risk of SWI. The Weight value (*W*) was assigned based on the pairwise analysis, see next section 4.2.2.

All parameter maps were produced in the Geographic Information System (GIS), and output result from Map-counting (Mc) analysis was imported to ArcGIS. In order to properly acquire consistency in the vulnerability index calculation, the parameter maps (thematic layers) were saved with a specified resolution (10 m) as a raster data. Ultimately, the vulnerability maps (vulnerability calculation) were produced using the sum cell statistics tool within ArcGIS.

1) Well density (W)

Well density (W) map shows the distribution of wells in an area. The point density tool was used to develop a well density map (density of wells per grid cell) from the wells data (well location information). In order to identify the influence of wells which are mainly dependent on the fractured bedrock aquifers, i.e., drilled wells were used. The output result of the well density calculation was divided into five groups based on the intensity of wells, using the unique values symbology setting in ArcGIS (Table 3). The rating value (1-5) was allocated to each group, i.e., high well density area (high water use) (5) and low or no wells areas (1).

The number of well significantly affect the water table of aquifers with the increasing demand of water. In general, an over-pumping condition in coastal aquifer results in a shift of the saltwater and freshwater interface further inland (Klassen et al., 2014). Thus, areas with a high number of wells have a high risk of SWI.

2) Elevation (E)

A relief map shows a slope variability of the land surface. LiDAR-based 2m resolution elevation model (DEM) was used to classify the elevation distribution of the study area. In ArcGIS, the customize unique symbols operation was used to classify the elevation data into five classes. Rating value from 1 (high elevated area) to 5 (low relief areas) was assigned to each class. The elevation of the study area ranges from -0.52 m a.s.l (above sea level) (highest rate value) to 58.35 m a.s.l 1 (lowest rate value) (Figure 13).

Topographic variation influence groundwater flux, which results in a change in the freshwater-saltwater interface. Steep slope areas increase groundwater flow from land to sea against density-driven flows of saline water from the sea to land (maintaining the interface close to the sea). By contrast, low slope areas have lower groundwater flow towards the sea that may result

in a further shift of the interface landward. In other words, the slope of an area influences the gradient and direction of flow, i.e., water column heights increase with elevation (Aller, 1985; Eriksson et al., 2018).

3) Lineament length (L)

Lineament length (L) factor refers to the extent (length) of dykes, deformation zone, and other structural formations. The length of the lineaments was calculated using the calculate geometry tool and grouped into five groups based on their length within ArcGIS. Each group was rated from1 to 5 to represent minor and major lineaments, respectively (Table 3).

The length of lineament (fracture) is generally related to the hydraulic conductivity of an aquifer. Major lineaments are often highly dissected by minor fractures, i.e., increase the number of hydraulic conduit (flow of groundwater or saline water) (Denny et al., 2007). In the Koster Islands, the structural setting is dominated by fractures associated with dyke swarm and regional deformation zones. Based on the length of lineaments, major lineaments (e.g., deformation zone) were considered to have a high risk of SWI.

4) Distance to the sea (D)

Distance to the sea (D) was determined using the Euclidean distance tool in ArcGIS, and the coastline was used as a reference polygon. The coastline polygon was extracted from the overview map (GSD-General Map) (Table 1). The study area was classified into five categories based on the distance to the coast calculation and given a rate value (1-5) (Table 3). The risk to SWI is higher in areas closer to the coast as the proximity to freshwater-saltwater interface decreases, and the interface is shallower near the shoreline. Thus, the probability of SWI decreases with increasing distance from the shoreline (further inland) (Kennedy 2012).

5) Lineament density (Ld)

Lineament density (Ld) map shows the distribution of lineaments per km^2. Lineament density was calculated using the line density tool in ArcGIS and clustered in 5 groups. Each group was assigned rate value ranging from 1 to 5, similar to the other parameters (Table 3). The hydraulic conductivity has been positively correlated with lineaments (fractures). Thus, areas with intensive lineaments were assigned high rate value (high-risk of SWI) and by contrast areas with low density were rated low (low risk of SWI) (Surrette and Allen 2008; Surrette et al.,

2008). In the Koster Islands, areas with intense dyke and fractures were assumed to have high conductive coundits.

6) Map-counting (Mc)

The map-counting (Mc) method was adopted from Peternell et al. (2011), used it to quantify the inhomogeneity of lineaments patterns based on fractal geometry. This method is capable of identifying structural geometry and patterns such as schlieren, magmatic folds, faults, and dykes that the human eye cannot easily determine. For a more detailed description of the methodology and development of these techniques, the reader is referred to Peternell et al. (2011).

The Mc method is an automated box-counting technique, where a specified sized box (white square) glides in two orthogonal directions at a constant distance (r) over the input lineament distribution map and analyses how each lineament fills the space. i.e., measure the degree of complexity (Figure 10). This method was modified to an automated box-counting (gliding window) analyzer to capture the complexity variation in the input data. The inhomogeneity of the lineaments is displayed in different colors, where each color reflects a specific inhomogeneity value (a positive real number D_b) (Peternell et al., 2011).

The output color-coded map (Figure 17) from the map-counting analysis was georeferenced and imported to ArcGIS, and a rate value from 1 to 5 was allocated based on the color distribution, and a weight of 5 was assigned (Table 3). On this study, the blue-green colored was assigned as low-risk areas, and red-yellow colored was assigned as high-risk areas. This classification was based on the relation or similarity of the map-counting results with the sector division of the Koster archipelago, based on the alteration and deformation degree (Figure 22) (Hageskov, 1985). Where highly deformed dykes (Sector III) aligns with low D_b value (blue-green colored) and moderately deformed (Sector II) aligns with high D_b value (red-yellow). Generally, the deformation level and alteration of formation are highly related to the conductivity of fractures, i.e., act as a hydraulic conduit (Surrette and Allen 2008; Surrette et al., 2008). Thus, it is assumed that highly altered and deformed dykes are likely to have high conductivity, i.e., high risk of SWI.

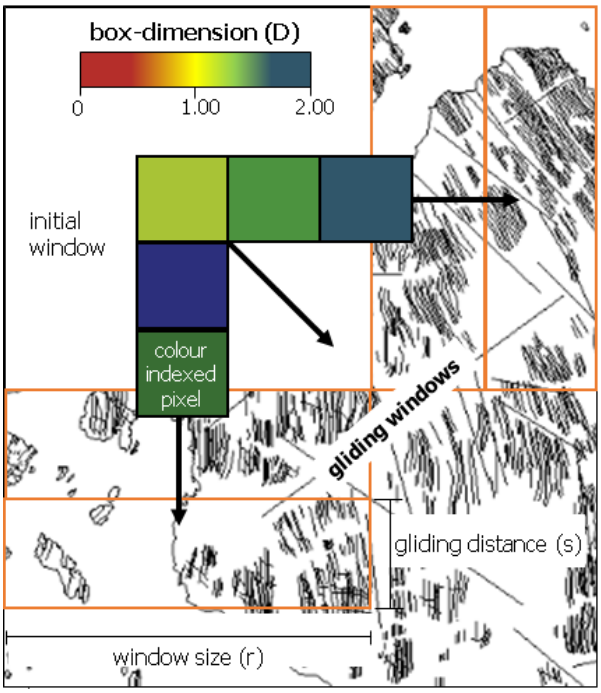

Figure 10 Map-counting method modified after (Peternell et al., 2011). A specified sized window (white square) glides in two orthogonal directions in a constant gliding distance (s) over the lineaments. The analyzed lineaments within every single square are plotted in the center of each window as a color-indexed pixel (D_b values)

4.2.2. Weight assignment

The Delphi method is a common approach in determining the numerical weights and rating value in a vulnerability assessment (e.g., Aller, 1985). The Delphi technique uses information acquired from experts to assess levels of risk. In other words, experts and scientists are surveyed to estimating the relative influence level of a parameter to the overall vulnerability of an area, e.g., strong influence means high weight value (Rahman, 2008).

In the present study, a pairwise analysis was conducted for determining the weight value of each parameter (Table 2). Previous studies and comments from experts were used as background information in performing the pairwise analysis. The weights of each parameter are ranked from 1 to 5, based on their significance (Aller et al., 1987). The number 0 in the table means the parameter in row *i* is less important than the parameter in the column *j*, and 1 means the parameter in row *i* is more important than the parameter in the column *j*, (*i*, *j*=1, 2, 3, 4, 5).

Table 2 Pairwise comparison analysis

Parameters	***W***	***E***	***L***	***D***	***Ld***	***Score***	***Rank***	***Weight Value***
W	-	1	1	0	0	2	3	3
E	0	-	0	0	0	0	5	1
L	0	1	-	0	0	1	4	2
D	1	1	1	-	0	3	2	4
Ld	1	1	1	1	-	4	1	5

W: Well density; E: Elevation; D: Distance to the sea; L: Lineament length; and Ld: Lineament density

4.2.3. Workflow

Figure 11 shows a simplified workflow scheme for evaluating the vulnerability of the Koster Islands to SWI and consists of the following major steps:

1) Identification of criteria representing geological features, geomorphological, and physical processes of the Koster Islands, which influence the flow of saline water or groundwater
2) Reclassification of initial data in order to assign rating value based on the influence of each parameter
3) Assigning weighting value to each parameter using pairwise comparison (Table 2)
4) Calculation of vulnerability index and developing aquifers vulnerability maps
5) Validation and comparison with surveyed data (observation data)

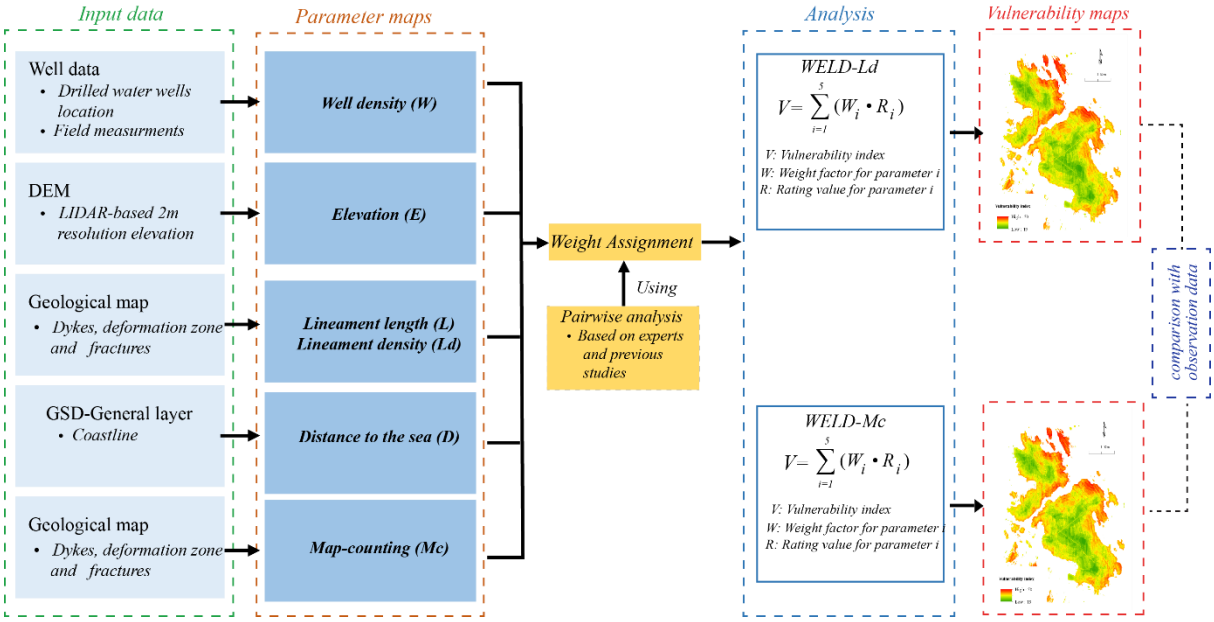

Figure 11 Flowchart of aquifer vulnerability mapping of Koster Islands

5. Results

Five thematic maps were prepared to represent each parameter in ArcGIS platform, and additional maps were created from the heterogeneity analysis (Mc) of the lineaments. The resulting parameter maps are presented in each section, including the vulnerability index value, classification range, and input data. Table 3 presents the assigned rate value (1-5), weight value (1-5), and vulnerability index results The vulnerability index reflects the risk of SWI, i.e., a high vulnerability index value (red color) represents a high risk, and a low vulnerability index (green color) represents a low risk.

Table 3 Parameters used in this study including classification range, rate, and weighting value and evaluated vulnerability index

Parameter	***Range***	***Rate Value (R)***	***Weight Factor (W)***	***Vulnerability index (V)***
Distance to the sea (m)	0 - 50	5		20
	50 -150	4		16
	150 – 250	3	4	12
	250 – 500	2		8
	500 – 1000	1		4
Lineaments Length (m)	0 – 200	1		2
	200 – 400	2		4
	400 – 600	3	2	6
	600 – 1600	4		8
	1600 – 3600	5		10
Lineaments Density (km²)	0 – 5	1		5
	5 – 25	2		10
	25 – 45	3	5	15
	45 – 65	4		20
	65 – 85	5		25
Well Density (wells per m²)	0	1		3
	0 – 50	2		6
	50 – 150	3	3	9
	150 – 250	4		12
	250 – 500	5		15
Elevation (m a.s.l.)	0 – 5	5		5
	5 – 10	4		4
	10 – 15	3	1	3
	15 – 25	2		2
	25 – 60	1		1
Map-counting	0	1		5
	3	2		10
	3 – 6	3	5	15
	6 – 9	4		20
	9 – 15	5		25

5.1. Parameter Maps

1) Well density (W)

Figure 12 (a) shows drilled wells (input data) and (b) well density map (W) of the Koster Islands. In the study area, well distribution is highest in the southwest part of North Koster. Relatively, drilled wells in South Koster is scarce and mainly situated in the southeastern tip (Figure 12, a). Generally, numbers of wells are directly related to the distribution of the population in the islands, i.e., high well density indicates areas with a high number of houses. Most of the drilled wells in the Koster Islands are located near the coast.

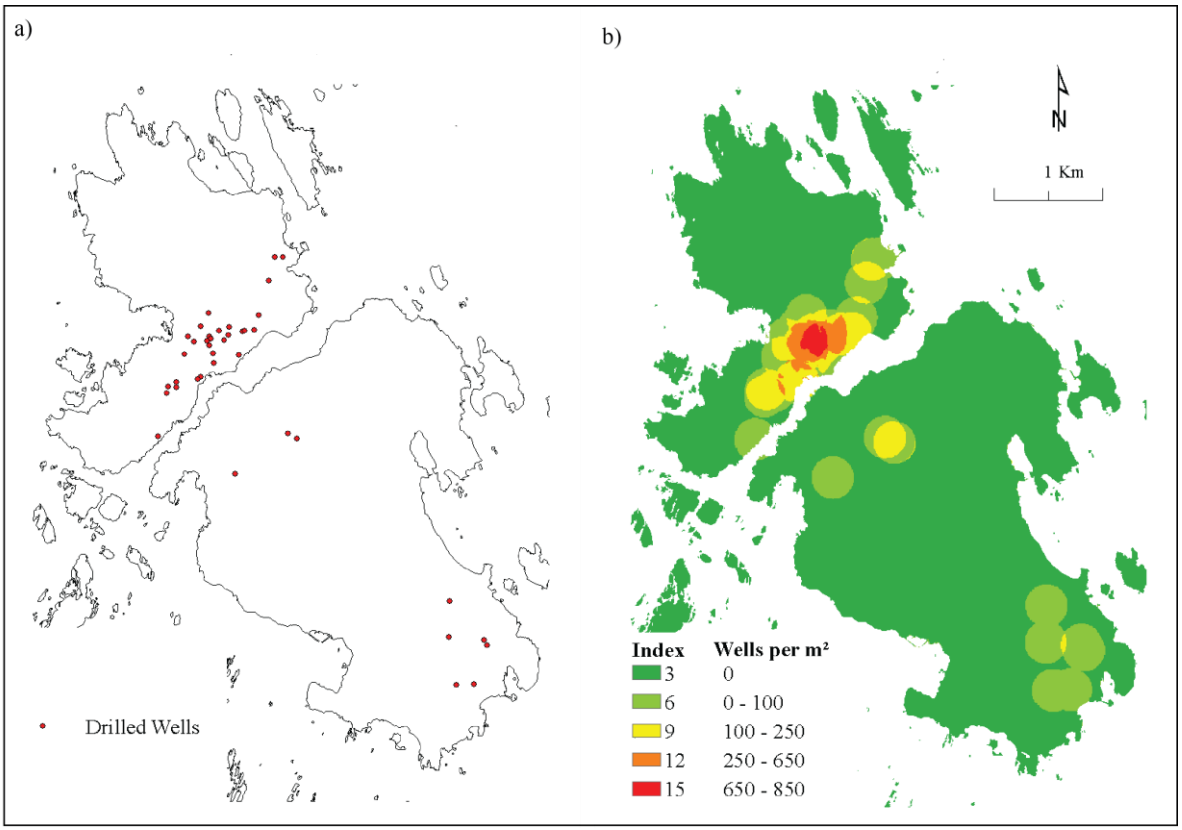

Figure 12 (a) Spatial distribution of drilled wells, (b) Well density map (W). The risk value (vulnerability to SWI) ranges from high-risk (red color=15) to low-risk areas (deep green=3)

2) Elevation (E)

The elevation of the study area ranges from - 0.5 to 53.35 meters above sea level (m a.s.l). In general, low-lying areas dominate most of the areas near the coastline, while elevation increases further inland. However, low-elevated areas are also situated further inland, and relatively high areas also dominate the coastal area. Figure 13(a) shows the original input elevation data (LiDAR +2m) and (b) depicts the topographic distribution based on the calculated vulnerability index.

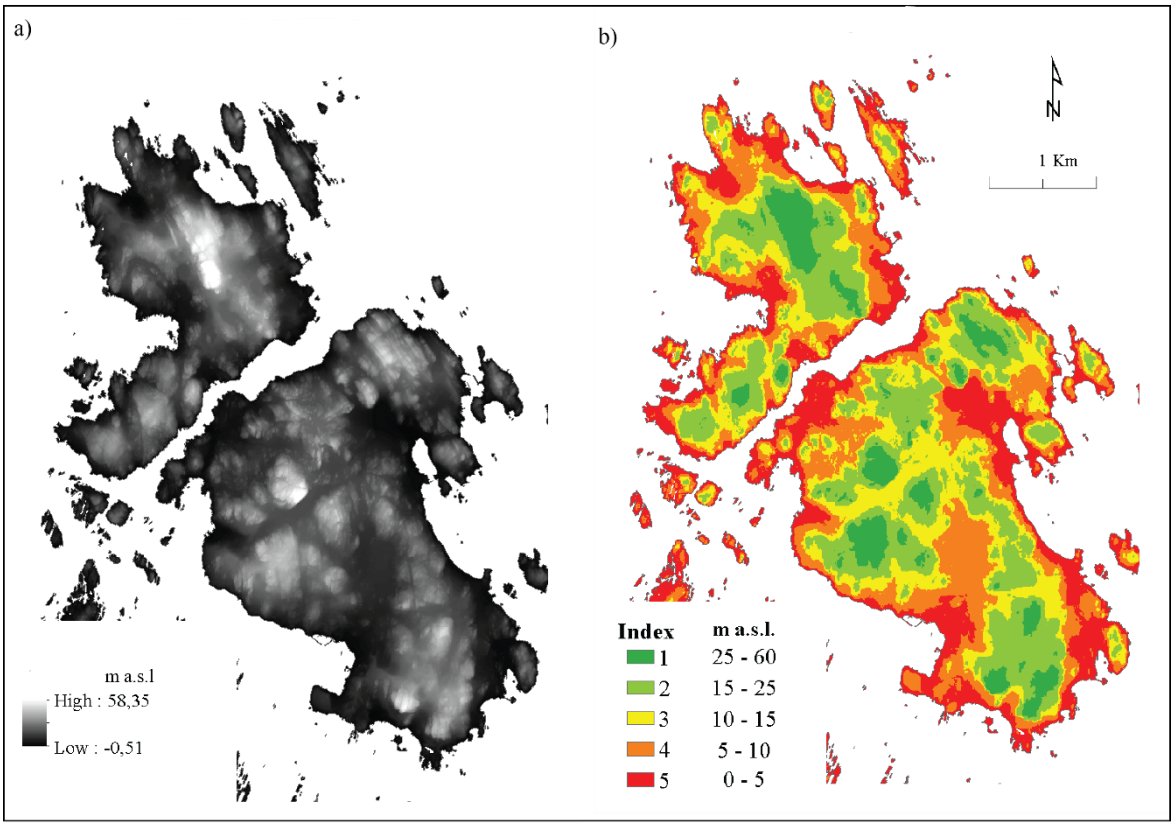

Figure 13 (a) DEM elevation data, (b) Elevation (E) map. The risk value (vulnerability to SWI) ranges from high-risk (red color=5) to low-risk areas (deep green=1)

3) Lineament length (L)

Figure 14 presents the lineament length measurement and vulnerability index values of lineaments in the study area. The length of lineaments varies between 0.5 m to 3600 m, where the major structures are deformation zones. These deformation zones are foremost in the South Koster Islands with NW-SW and NW- SW orientation. The dominant opening and fractures (dyke swarm) have an N-S orientation. The vulnerability index evaluation shows that the majority of the lineaments have moderate (deep green – light green) vulnerability index.

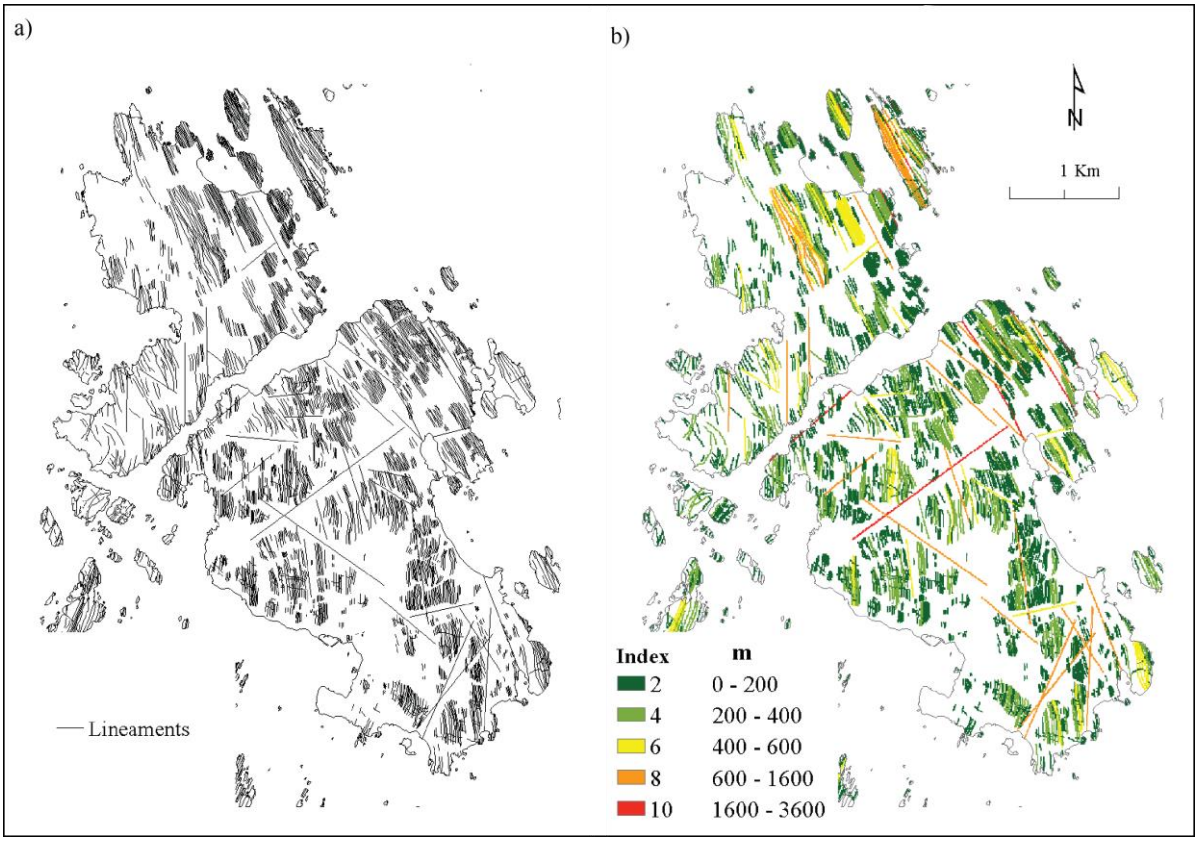

Figure 14 (a) Lineament map, (b) Lineament length (L) parameter. The risk value (vulnerability to SWI) ranges from high-risk (red color=10) to low-risk (deep green=2)

4) Distance to the sea (D)

Distance to the sea (D) shows the risk of areas based on the distance to the shoreline. Figure 15 (a) shows the coastline of the Koster Islands and (b) the calculated distance to the sea with its corresponding vulnerability index. Based on the distance to the coast calculation, South Koster aquifers have low-risk area coverage compared to North Koster. The distance to the sea (D) map shows a homogenous change shifting from high-risk to low-risk from the shoreline to the land, with the highest risk areas are situated near the shoreline (0 – 50 m).

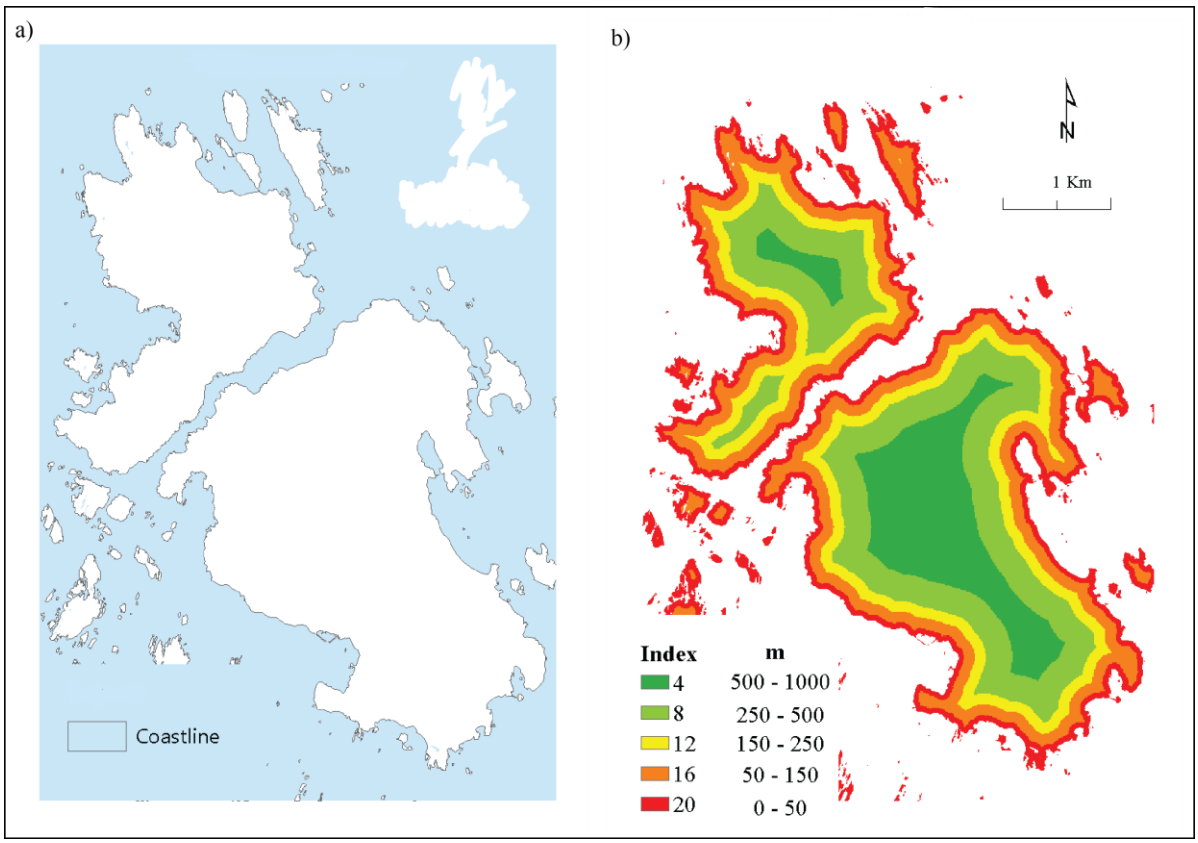

Figure 15 (a) The coastline of Koster Island, (b) Distance to the sea (D) map. The risk value (vulnerability to SWI) ranges from high-risk (red color=20) to low-risk areas (deep green=4)

5) Lineament density (Ld)

The lineament distribution is higher on in South Koster compared to North Koster (Figure 16). On North Koster, the lineament density is dominant in the northeast part of the island; while on South Koster lineaments are generally evenly distributed throughout the island with predominance in the northeast part. In the vulnerability assessment for the Koster Islands, lineament density has the most influence on aquifer vulnerability (Table 3).

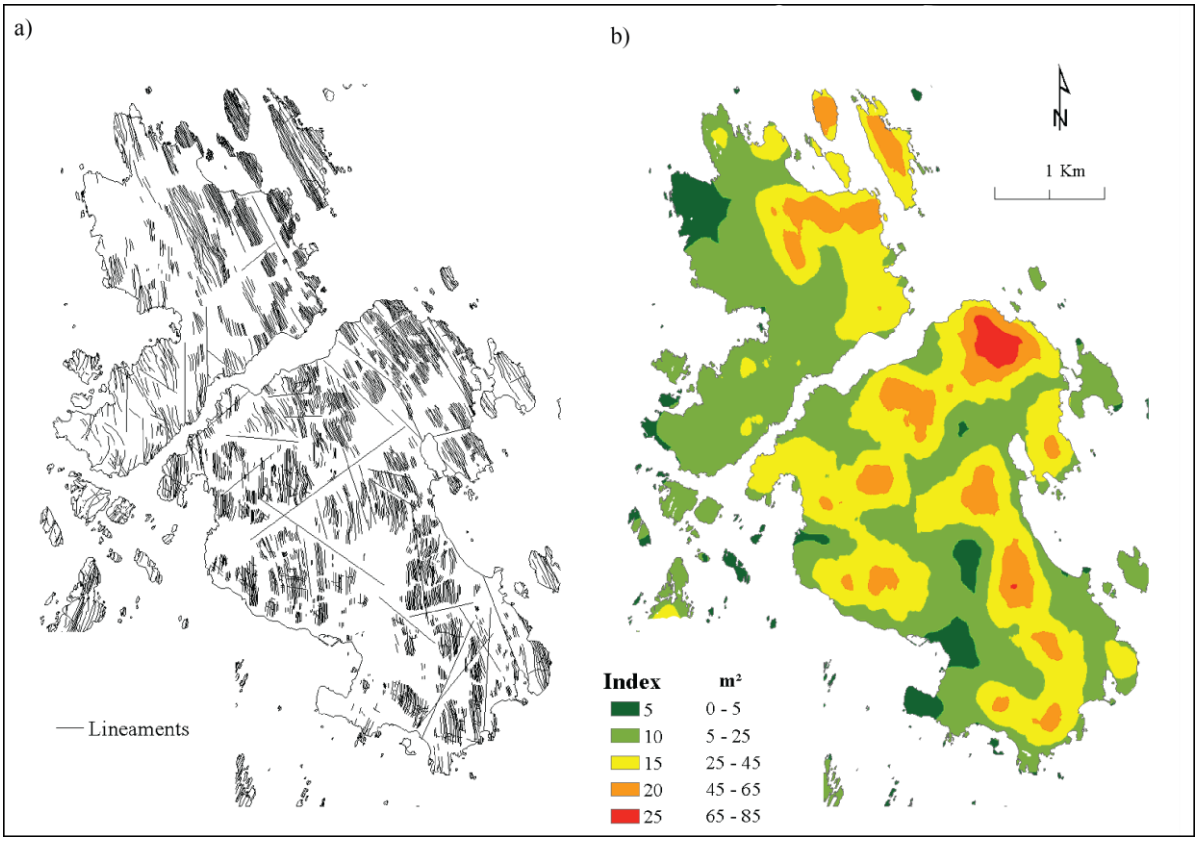

Figure 16 (a) Lineament map, (b) and Lineaments density (Ld) map. The risk value (vulnerability to SWI) ranges from high-risk (red color=25) to low-risk areas (deep green=5)

6) Map-counting (Mc)

Figure 17 presents the results acquired from the inhomogeneity quantification of lineaments distribution (Figure 16, a) and the Mc parameter map. The color-coded Mc map (Figure 17, a) shows the inhomogeneity degree of the lineaments. The color-coded map of box-counting value, i.e., D_b value ranges from 1.6 (blue-green colors) to 1.9 (white-yellow colors). The range of values represents the lineaments inhomogeneity (complexity) (Peternell et al., 2011). The D_b values of Koster Islands lineament pattern shifts from northeast (1.6) to southwest (1.9). The resulting box-counting map of North Koster is dominated by low D_b values ranging from ~ 1.6 (blue) to ~ 1.7 (green) with minor areas with high D_b value (~ 1.75 to ~1.85) in the W-SW part. South Koster is divided into two sections, where the SW part of the island displays high D_b values (~ 1.8 to ~1.9) with scattered blue color (~1.6), and the NE part of the island shows ~ 1.6 (blue) to ~ 1.7 (green). A high vulnerability index value, i.e., low D_b value corresponds to highly deformed and altered dyke swarm in the N-NE part of the islands. The S-SW part of the island with high D_b value assumed as a low-risk area (less susceptible to SWI).

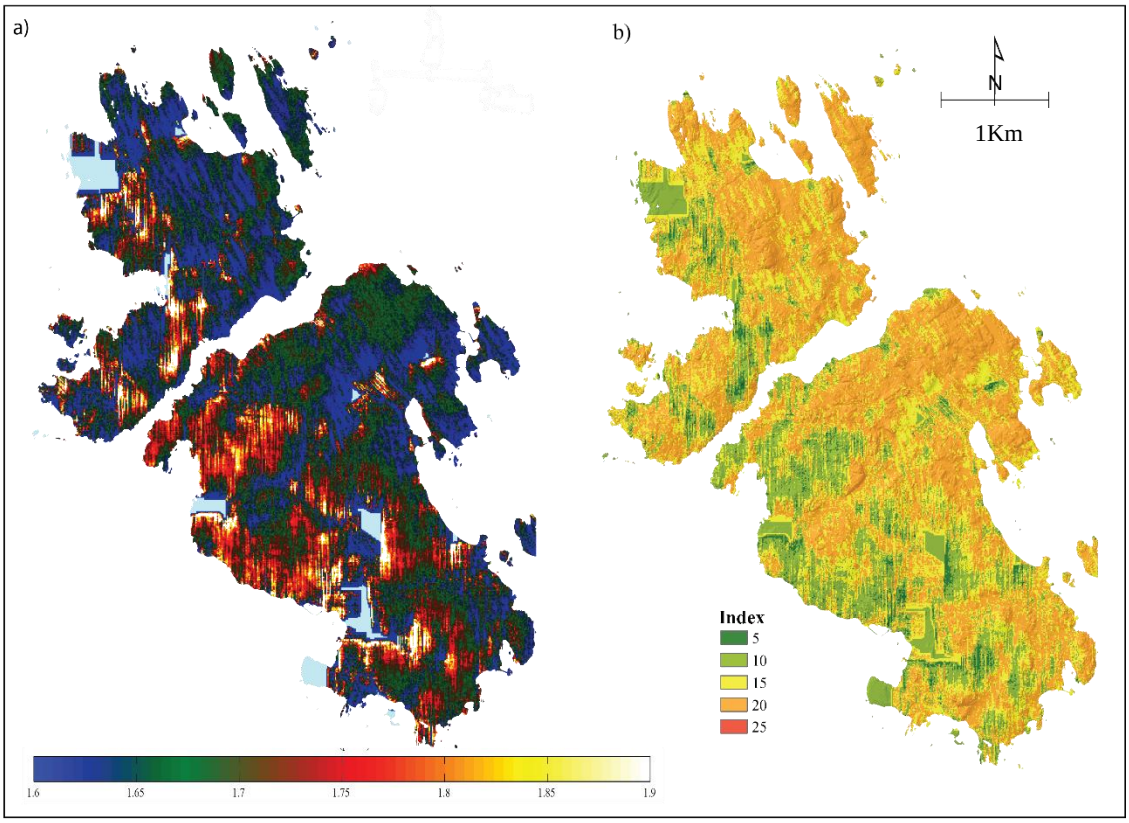

Figure 17 (a) Result of the map-counting analysis, (b) Map-counting parameter map (Mc) The vulnerability index value ranges from high-risk (red color=25) to low-risk areas (deep green=5)

5.2. Aquifer vulnerability map

The vulnerability map is the combined result of all parameter maps. Figure 18 shows the susceptibility map created using the WELD-Ld model, and Figure 19 depicts the result of WELD-Mc model. These vulnerability maps display the spatial distribution of the risk of SWI on the Koster Islands. The vulnerability index of the study area extends from high (red color) to low (green color) risk of SWI. The output of the WELD-Ld and the WELD-Mc model (Figure 18; Figure 19) identifies vulnerability index of the study area ranging from 16 (low) to 58 (high) and 13 (low) to 60 (high), respectively.

The WELD-Ld model results revealed that the north-eastern part of the islands is highly susceptible to SWI, compared to SW and NW parts of the islands. Areas of moderately high to high vulnerability (yellow-red; Figure 18) exist primarily at the periphery of the islands and in areas of high intense lineaments (fractures). The WELD-Ld model is quite sensitive to the density of the lineaments (Ld) and proximity to the coastline (D). Also, a high density of wells (W) in the south and southwest part of North Koster considerably increase the SWI risk.

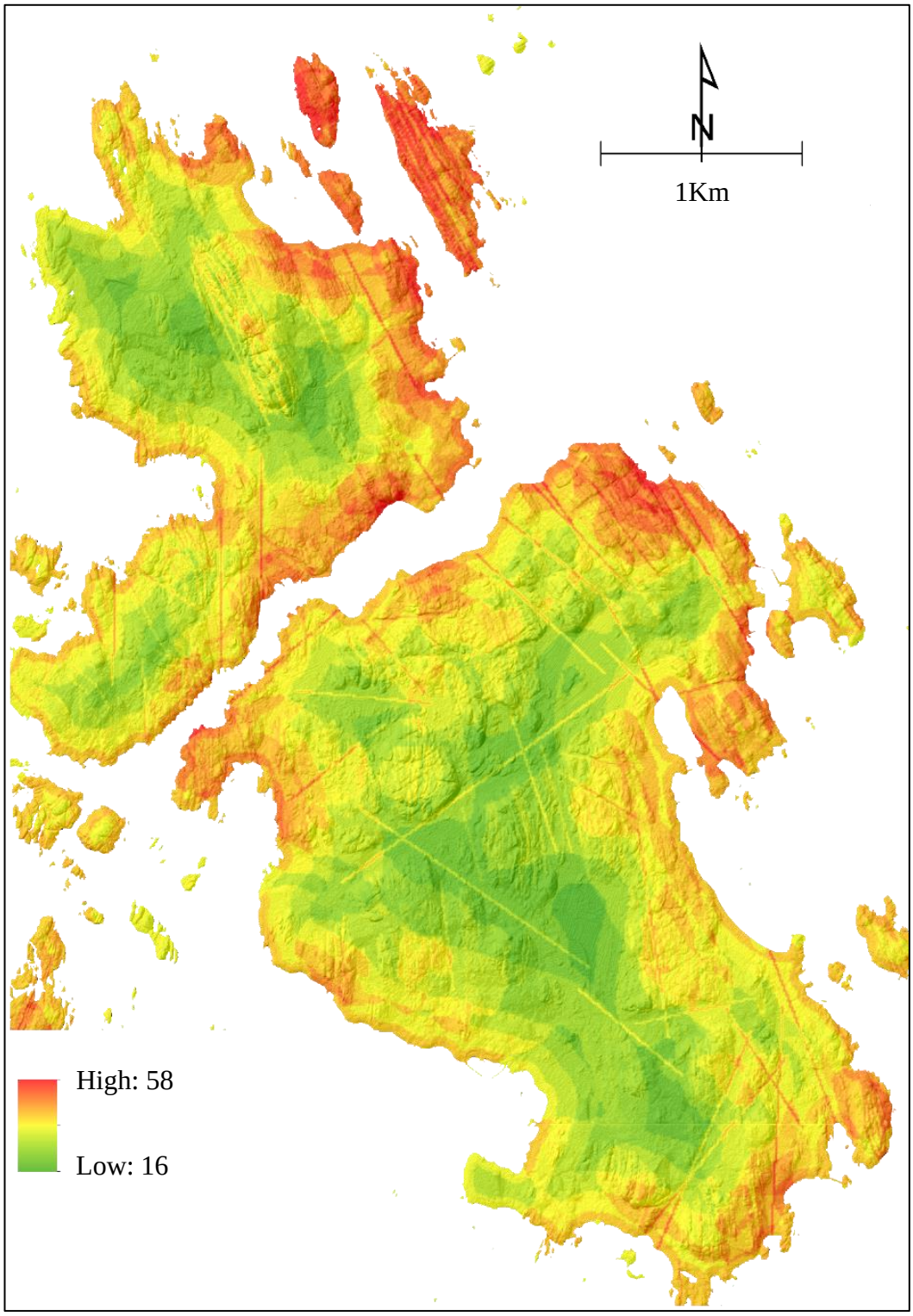

Figure 18 WELD-Ld model result

The WELD-Mc aquifer vulnerability map (Figure 19) shows that the shoreline areas of the study area have a high vulnerability, and most central parts of the islands have a low-moderate vulnerability (green-yellow). Areas with moderate-high exist primarily at the north-northeast where the inhomogeneity value (D_b) lineaments are low (Figure 17) in areas of highly altered

and deformed dyke swarm. High-moderate vulnerability trends also precede along major lineaments, including further inland areas. This is particularly evident on the central and south portion of South Koster due to the presence of major lineaments (e.g., deformation zone).

Comparing the WELD-Ld and WELD-Mc results (Figure 18; Figure 19), the overall impact of the Mc parameter results augmented the vulnerability of the islands fractionally; however, several parts also depict relatively lower risk. The total amount of the vulnerability index remains constant, by the spatial distribution changes. The decrease of (D_b) value in the NW-SW part of the islands within low-moderate index (green-yellow) areas (Figure 17), slightly increased the vulnerability index to moderate (yellow; Figure 19). This is particularly evident in the center and northwest part of North Koster. By contrast, on the northeast portion of South Koster, the vulnerability has reduced from high-risk areas (red areas) to moderate- high (yellow-red). Also, there is a notable increase of susceptibility in the northwest of North Koster in the WELD-Mc results.

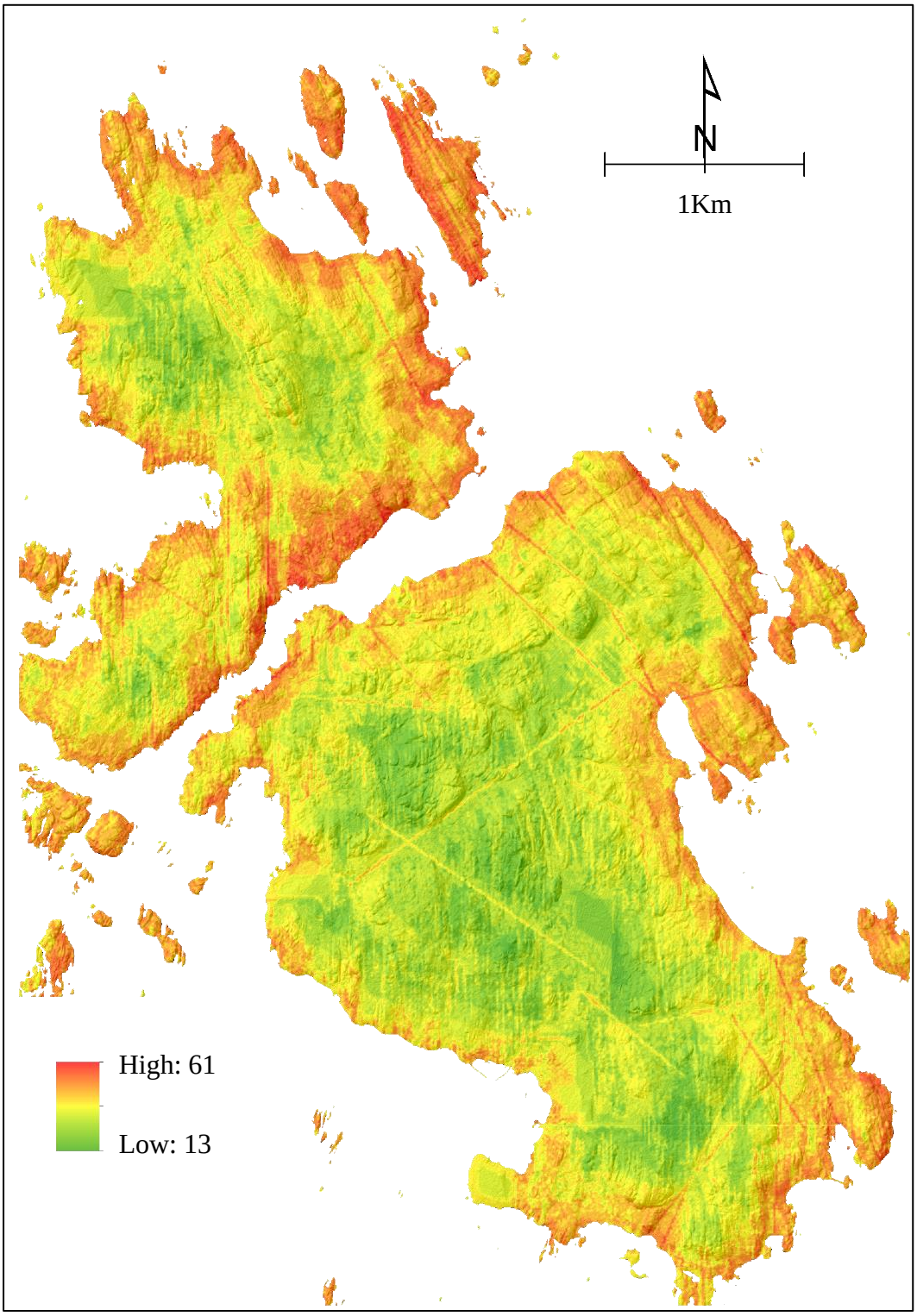

Figure 19 WELD-Mc model result

5.3. Comparisons with measured data

Validation of the vulnerability assessment results using measurement data is an effective way to correlate qualitative measurements (e.g., electric conductivity) with vulnerability maps. Chemical analysis and electrical conductivity (EC) measurement data of drilled wells were

acquired from previous studies conducted in the Koster Islands. The analyzed groundwater samples are not depth-specific instead collected from observation wells and domestic water outlets (house taps). For spatial comparison, the EC and Cl concentration measurements samples from July and September-2016 were overlain on the WELD-Ld and WELD-Mc model results (vulnerability maps). The samples from July and September were selected because during these months a high number of tourists visit Koster Islands and less precipitation occur. Thus, it is useful to identify wells at risk during high-stress periods, i.e., high groundwater demand and low groundwater recharge. The samples were grouped into classes ranging from I-V based on the SGU groundwater quality assessment classification (scale and range) (Table 4; SGU, 2013).

Table 4 Groundwater standard quality assessment scale and range from the SGU. Blue color (Class I) represents low concentration or relatively suitable water while red (Class V) represents high concentration values and not suitable water for drinking

Parameter	*Class I*	*Class II*	*Class III*	Class IV	Class V
Electrical conductivity (mS/m)	*<25*	25 - 50	50 - 75	75 -150	≥150
Chloride (mg/l)	*<20*	20 - 50	50 - 100	100 - 300	>300

According to the samples from July, a large percentage of wells are categorized as class II, III, and IV. In September the majority of the wells lies in class II and class III. The EC and Cl measurements, especially from July (Figure 20) depicts similar trends, particular class IV wells in the North Koster and the southernmost tip of South Koster. Majority of class IV and V wells lie along the coast and near major lineaments in areas mapped as moderately high to high vulnerability (yellow and red). However, there are some inconsistencies; for example, wells in the southeastern part of North Koster have low Cl values (Class II) (Figure 20). Low values of EC and Cl could be explained by the heterogeneous nature of the fractured aquifers, i.e., the distribution and conductivity of the lineament may locally influence individual wells. Thus, high conductive fractures may act as conduits for freshwater as well as saline water.

Regarding the correlation between well depth and measured data, it can be seen that there is no strong correlation between well depth and Cl and EC values. During July high EC and Cl (class IV) measurements are observed in wells with 0-250 m depth and one well >500 m depth in North Koster (Figure 20). In September high EC (class IV-V) were recorded in 4 wells with varying depth and low value (class II) dominant in wells with 50-250 m depth (Figure 21).

Comparing the WELD-Ld and WELD-Mc model with the measured data. Relatively the vulnerability estimation of the WELD-Mc model is consistent with measured data, especially with July measurements and wells in South Koster (Figure 21). However, there is no significant difference, both WELD-Ld and WELD-Mc results show almost similar spatial distribution of the risk of SWI.

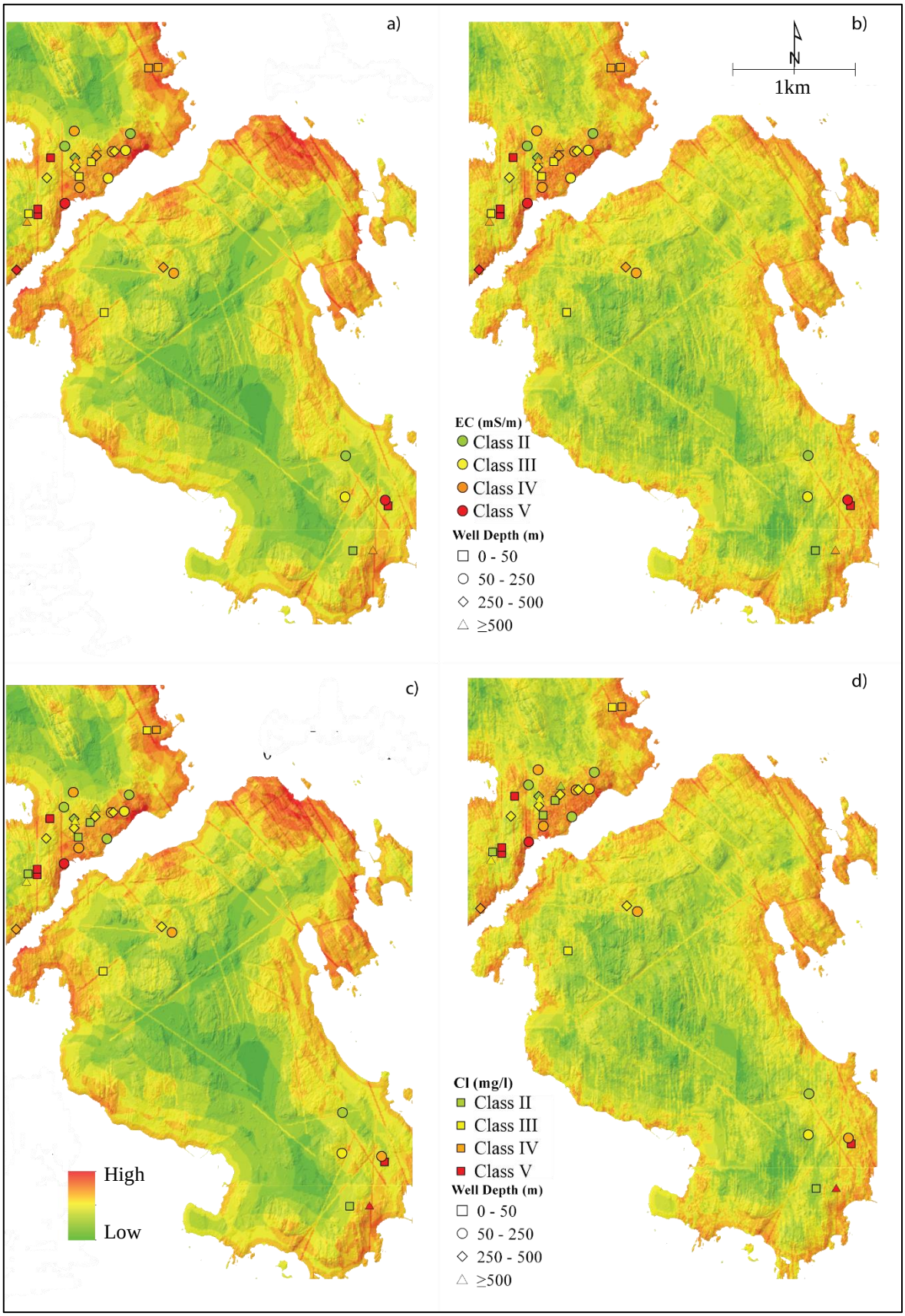

Figure 20 July-2016, EC (a; b) and Cl (c; d) - measurements in drilled wells (a; c) WELD-Ld and (b; d) WELD-Mc

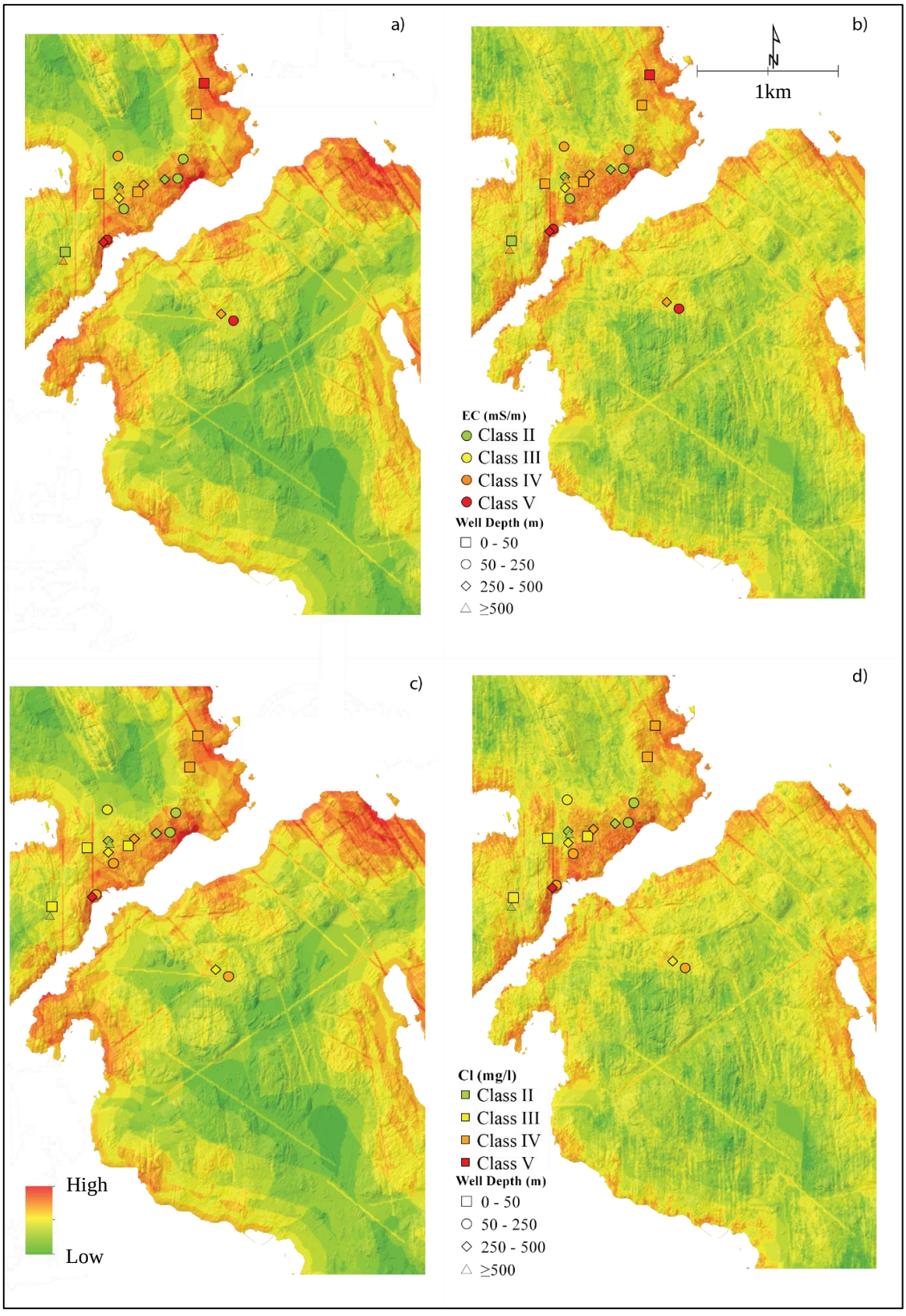

Figure 21 September-2016, EC (a; b) and Cl (c; d) - measurements in drilled wells (a; c) WELD-Ld and (b; d) WELD-Mc

6. Discussion

The focus of this paper is twofold: (1) to provide a review of the current understanding of SWI and methods used to investigate SWI, with a focus in fractured crystalline-rock aquifers, (2) to develop aquifers vulnerability maps, i.e., estimate the degree of susceptibility of Koster Islands aquifers to SWI.

The present study encompasses the following main concepts and evaluations:

- Processes and drivers of SWI
- Methods used for analysis and monitoring SWI
- SWI in Sweden (Scandinavian) with a focus in fractured bedrock aquifers
- Evaluation or estimation of risk of SWI of Koster Islands aquifers
- Inhomogeneity quantification (map-counting) of Koster Islands lineaments (fractures)

6.1. Previous studies

The literature review section presents the current understanding of SWI and summarizes the approaches used in analyzing the flow of groundwater in the sophisticated setting of fractured bedrock aquifers. Based on the literature review, the current study shows that there have been significant advances in SWI monitoring, data processing, and modeling over the past decade. However, the understanding of SWI in a fractured crystalline-rock aquifer is incomplete and challenging.

In Sweden, SWI has been considered as a single well problem, but with the increase of SWI cases has raised awareness from the local scale up to municipalities level. However, more research and assessment are recommended to understand the hydrogeological nature and mechanism of SWI to manage and avoid further contamination of wells or aquifers.

6.2. Aquifer vulnerability map

The aquifer vulnerability map shows that the most vulnerable areas in the Koster Islands are along the shoreline, mainly in the north-northwest parts of the islands while lower vulnerability prevails along with the central, southwest and northwest parts of the islands (Figure 18; Figure 19). However, the entire Koster Islands shows a risk of salinization to some degree, with the lowest vulnerability index value of 13 (WELD-Ld) and 16 (WELD-Mc). The risk of SWI along

the coastline has been an everyday challenge in many locations around the world, and it is mainly related to the increasing number of housing along the coast, population growth and tourism (Cashman et al., 2010; Ranjan et al., 2009). It can thus be suggested that future development planning on the Koster Islands should take into account the risk of an increasing number of housing around the shoreline areas and risk of water security.

Among the influencing factors, lineament density (Ld) were significant in many parts of the islands and are considered as a dominant influencing factor on the vulnerability of the study area (Figure 16). A qualitative and quantitative study of fault-related permeability structures by Caine et al., (1996) concluded that fractures distribution changes with proximity to faults (major structures) is common, and strongly influence the fluid flow. In the study area, major lineaments (deformation zone) are not tectonically related to the dyke swarm, and the present lineament map (Figure 14, a) is limited to display the correlation between deformation zones and change of fracture distribution. In accordance with the present results, densely distributed, altered and strongly deformed rocks (Koster dyke swarm) as the result of NW-SE-trending shear zone (Hageskov, 1985), maybe have a higher risk of SWI due to the possible increase of permeable conduits. This assumption aligns with an earlier study conducted by Caine et al., (1996), which showed that permeability of fracture depends, on the geological formation and degree of alteration (i.e., highly altered corresponds to high permeability). Also, the Mc map (Figure 17) showed that the fractal geometry of the dyke swarm in N-NE (highly altered and deformed dyke rocks) of the islands shows unique characteristic compared to the S-SW parts.

The mapping of the Koster lineaments, such as the dyke swarm is based on LiDAR and aerial photographs. However, this technique of mapping has several limitations. Research such as that conducted by Scheiber et al., (2015) has shown that three factors, i.e., scale, illumination azimuth, and operator influence the output lineament maps, such as number and length of lineament. In this study, the lineament map (Figure 14, a) may create a potential bias or alter the calculation of the parameters (e.g., Ld). Structural information (e.g., maps) derived from LiDAR and high-quality satellite images are limited in estimating the extent of the lineaments below the ground surface and only represent the surface expression of the ground surface, i.e., only outcrop structures. For example, fracture (lineament) density is the number of fractures per unit volume of rock. However, it is challenging to acquire such information both technically and economically, especially in large scale.

Nevertheless, detailed local scale assessment (e.g., distribution of water resources) and conceptual model of lineaments are essential methods that can be used to capture detailed fracture information (e.g., estimate permeability variations) and decreases uncertainty (Denny et al., 2007). To develop a full picture of Koster Islands aquifers, additional studies will be needed that can provide additional information on water-bearing rocks, structural setting, and their hydrogeological setting. Especially the results of Ld map is limited in capturing the lineaments density (fractures opening).

In the pairwise analysis well density (W) parameter was chosen over lineament length (L) and elevation (E) because extraction of freshwater most often affects the balance between freshwater-saltwater interface, thereby increasing risk of SWI (Barlow, 2003). In addition, Park et al. (2012) found that continuous intensive pumping is a major cause of SWI in a tidally-forced coastal fractured aquifer. One major drawback of the well density mapping is that the well information acquired from SGU is incomplete. In this study, only 39 wells were used in creating the well density map (Figure 12, a). However, 280 wells of 800 wells in the Koster Islands are known as drilled wells (Banzhaf et al., 2017). As a result, the well density map (Figure 12,b) may not estimate the actual density of the wells. Up to date wells archive, including well status information, would have been a valuable material in acquiring a reliable well density mapping, thereby increase the assessment accuracy.

In developing groundwater vulnerability map, a number of GIS-based multicriteria risk analysis methods, such as 'DRASTIC,' have been widely used in many parts of the world (e.g., Ebert et al., 2016; Eriksson et al., 2018; Neshat et al., 2014; Tangestani, 2009; Vias et al., 2005). The primary aim of this map is to estimate the relative susceptibility of areas to groundwater contamination based on hydrogeological and anthropogenic factors (Aller, 1985). However, it is clearly stated that groundwater vulnerability mapping, such as the DRASTIC and WELD-Ld method is not an alternative approach to replace field investigation (Aller, 1985). However, groundwater vulnerability map can be an efficient method for groundwater management when used in conjunction with field measurements. Nevertheless, studies conducted by Rupert (2001) have also argued that the results acquired from the DRASTIC model are inconsistent with actual measured data. However, he also concluded that the accuracy of this method could be improved by calibrating the rating value based on the acquired result (field measurements) instead of expert knowledge. Even though the models used in this study did adopt all the parameters form

DRASTIC model; however, a similar approach and vulnerability index calculations were adopted, e.g., rating range, hence similar limitations apply. It is also highly recommended to modify (update) the vulnerability map with changes (e.g., number of wells) that can considerably affect the susceptibility of aquifers. Assessment scale of the vulnerability maps could be another limitation. For detailed local scale (single wells) risk potential, it should be considered to conduct small scale survey (detailed analysis). The vulnerability maps, therefore, need to be interpreted with caution when used in a single well problem.

6.2.1. Comparison with measured data

Electrical conductivity result was compared with the acquired aquifer susceptibility maps. EC measurements are a fast and cheap approach to evaluate the amount of salt content in a water sample (section 2.3.2). Generally, the vulnerability maps results (WELD-Ld and WELD-Mc) aligned with EC results of the drilled wells (Figure 20; Figure 21). For example, most of the drilled wells situated near the shoreline and major lineaments displayed high EC. However, some wells show relatively lower values even though they fall in areas with high vulnerability; this can be interpreted in several ways. First, the heterogeneous nature of fracture aquifers is much complex, beyond the scope of the current work. Thus, the hydraulic conductivity of aquifers is affected by minor fractures, which influence the chemistry of water locally. Secondly, the amount of freshwater in the aquifers and withdrawal amount, e.g., several wells drilled in single aquifer, highly determine the interface position. Lastly, the accuracy of the EC measurements and sampling spot and sampling season may affect the EC measurements. Further hydrogeological investigation, such as long-term monitoring of water level and EC (Park et al., 2012), would have been crucial in understanding the causes of exceptional wells with high EC values.

Chloride concentration analysis is one of the common ways in analysis SWI, and chloride anion is common indicators of SWI and is used in monitoring coastal aquifers (section 2.3.1). Most of the time, high level of chlorite in coastal areas are most likely related to SWI (Klassen et al., 2014). In the Koster Islands, most of the wells that fall in the high vulnerability areas show high chloride concentration (Figure 20; Figure 21). Generally, high Cl concentration in wells is related to active SWI. However, contamination from relict saline water is also possible. In the case of the vulnerability maps, wells, which reflect low Cl values in lies areas that are estimated

to be high risk to SWI, a further assessment, could be helpful to verify and trace the primary source of Cl.

6.3. Map-counting (Mc)

The inhomogeneity quantification of lineaments (Mc map) showed that lineaments in N-NE parts of the islands have different values (D_b) compared to S -SW parts (Figure 17). This output map aligns with the previous study conducted by Hageskov (1985). For the ease of interpretation, the output map of the Mc analysis was integrated with a map of the sector division of the Koster archipelago based on the structural evolution of the islands (Figure 22).

Based on the dyke rocks deformation and transformation degree, Hageskov (1987) divided the Koster archipelago into three sectors (I, II and III and subsectors (A, B, C, and D) (Figure 22, a). Dykes in the sector I is relatively undeformed reserving the original igneous dolerites composition, in sector II dykes, are exposed to shearing and partly recrystallized to meta-dolerites, and in sector III B, C and D are also known as "the high strain belt" the dyke swarm are intense deformation and total recrystallized. This finding broadly supports the results from the present study, where the southwest part of the Koster archipelago is relatively less vulnerable with low (D_b) value, while Sector III (the high strain belt) highly vulnerable with high (D_b) value (Figure 22, b). This highly fractured dyke swarm is thus assumed to be the most influential hydrogeological factors in regulating the flow of water in Koster bedrock aquifer. This dyke swarm may act as conduits to provide a potential pathway for saline water to move into the aquifer. Despite these promising results, several questions remain unanswered. Further research should be undertaken to investigate the reason behind the similarity of the sector I and sector III. Also, further analysis of the lineaments of the Koster Islands (dyke swarm) would be essential to interpret the map-counting results in depth.

Studies conducted by Hodkiewicz et al., (2005) and Ford and Blenkinsop (2008) showed that fracture dimension analysis is an effective way estimate conductive conduits in fracture rock for hydrothermal fluid flow during the formation orogenic gold deposits. Also, conclude that high and low fractal dimensions (complexity gradients) correspond to the connectivity along fluid pathways in fractured bedrocks, e.g., higher complexity fractal diminution has the potential to transport large volumes of fluid. These studies further support the interpretation of

Mc calculation of the study area where the degree of complexity change with the deformation degree of the lineaments, which may have a high risk of SWI.

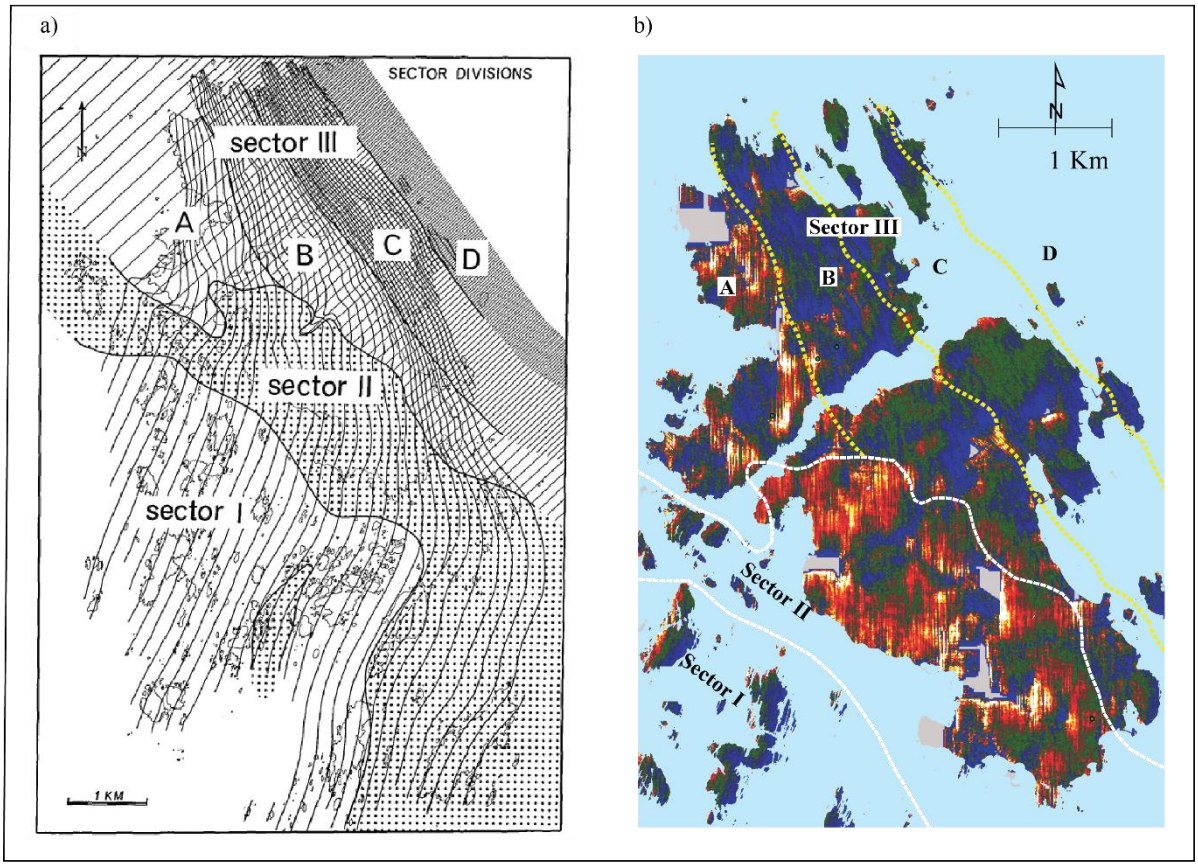

Figure 22 (a) Sector division of Koster Islands based on the deformation and alteration degree; (b) Map-counting result integrated with the sector division

7. Conclusions

In this study, the main aim was to assess the risk of SWI in a fractured bedrock aquifer of Koster Islands. A multicriterion GIS-based method and map-counting inhomogeneity analysis were used to assess groundwater vulnerability. Two vulnerability maps WELD-Ld and WELD-Mc were produced based on five parameters (well density, elevation, lineament length, distance to the sea, lineament density, and map-counting). The salient conclusions that can be drawn from this study are:

- The multicriterion vulnerability assessment deployed in this study found to be useful in estimating the risk of salinity in Koster Islands with readily available data

- Parameter weighting in the vulnerability assessment is a challenging task, because different judgments and scarcity of information may produce markedly different results; hence, the quantification accuracy is dependent on availability and input data accuracy

- Comparatively, North Koster aquifers are more vulnerable to SWI compared to South Koster. Particularly aquifers situated in northwest parts of the North Koster is relatively more vulnerable to SWI, which is mainly due to highly sheared and densely distributed dykes. While the west, northwest, and southwest parts of the islands are relatively less vulnerable to SWI (Figure 18; Figure 19)

- The presented vulnerability maps are ideal for use in future groundwater planning studies, where potential saltwater contamination may occur. The output results must not be the sole criteria and replace fieldwork in assessing salinity contamination. Thus, these maps with additional field surveys and detailed studies can be used as an efficient tool for groundwater management

- The inhomogeneity (map-counting) analysis of the lineaments shows that the northwest part of the Koster Islands have different inhomogeneity value compared to S-SW part of the islands (Figure 22, b). This inhomogeneity value (D_b) cannot be explained as a simple characteristic of the fractal geometry of the Koster dyke swarm. However, it is highly related to the tectonic process, which reshaped the Koster dyke swarm during the Sveconorwegian orogeny (Hageskov, 1987)

- In general, the comparison of observation measurements (EC and Cl measurements) and the final vulnerability maps depict a similar trend with few exceptional measurements. Most of the wells with high EC and Cl value fall within the high-risk areas

7.1. Recommendations

- Much progress has been made in understanding the processes behind SWI and developing assessment methods to monitor and managed aquifers in coastal regions. The geophysical approach is one of the approaches found to be useful in mapping SWI in complex geological environments. In the Koster Islands, geophysical survey (e.g., electromagnetic) would be an effective way to understand the hydrogeological setting of the aquifers as well as trace the saltwater-freshwater interface position

- A regular survey of the private well is an effective way to monitor SWI. For example, high-risk potential wells should be banned and shift to another location. As retrieving the original condition of an aquifers takes considerably long time and much more expensive than installing new wells

- Easy modification of the models used (e.g., include new parameters) is advantageous as this allows a user to update the model easily, and this may improve the accuracy of the output results (vulnerability maps). For example, fracture-network connectivity and orientation are some of the major factors that influence groundwater flow in fractured rock aquifer setting (e.g., Llopis-Albert and Capilla, 2010). In this study, a high resolution of anisotropy distribution maps of Koster lineaments was calculated side by side with the Mc analysis (Figure 23). However, this result was not incorporated with the current analysis due to the limitation of time and data. A further study with more focus on lineaments orientation and fracture-network connectivity is therefore suggested

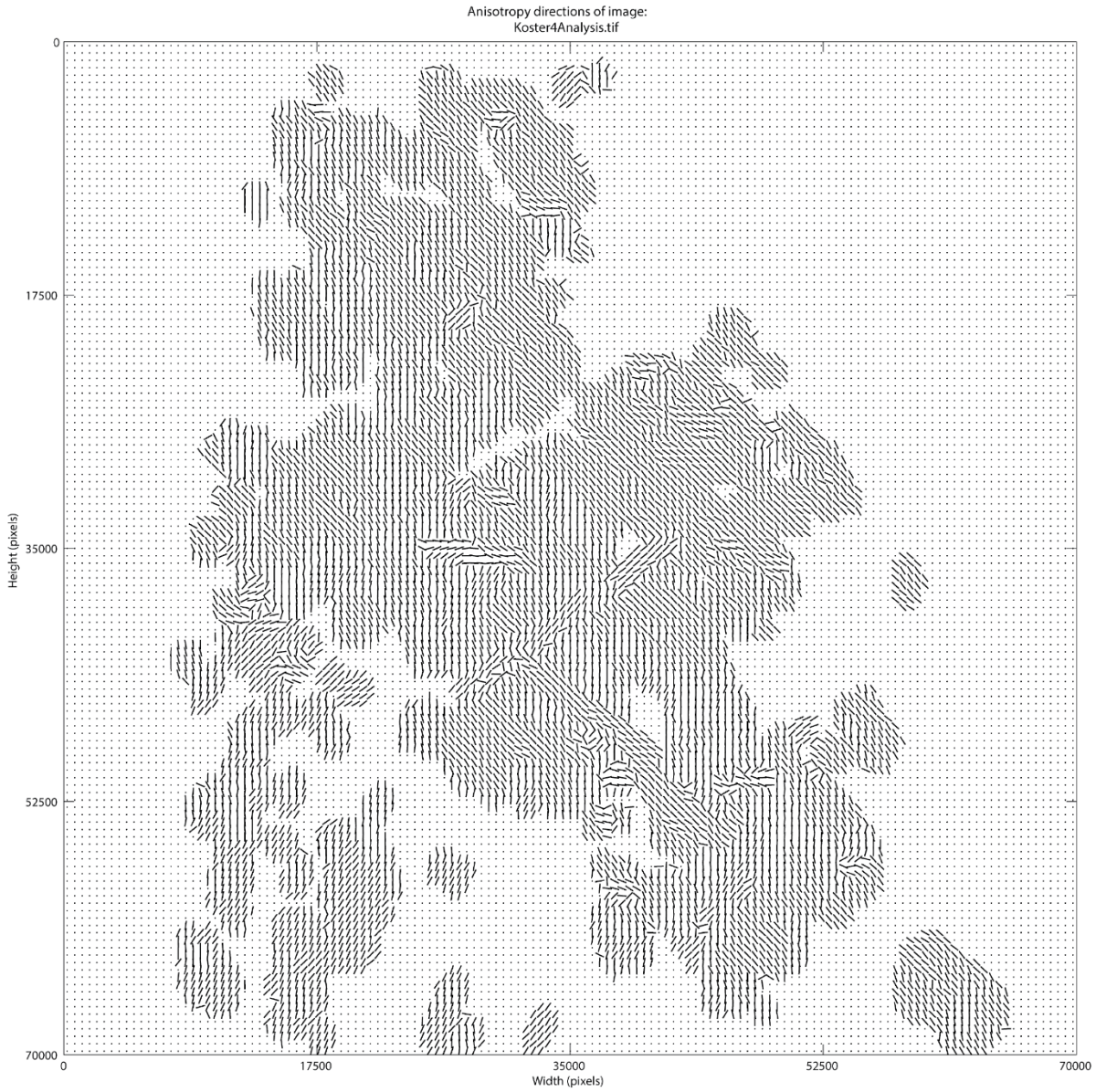

Figure 23 Result of the MORFA (Mapping of rock fabric anisotropy); anisotropy of the lineaments

References

Abarca, E., J. Carrera, X. Sánchez-Vila, and C. I. Voss, 2007, Quasi-horizontal circulation cells in 3D seawater intrusion: Journal of Hydrology, v. 339, p. 118-129.

Al-Adamat, R. A., I. D. Foster, and S. M. Baban, 2003, Groundwater vulnerability and risk mapping for the Basaltic aquifer of the Azraq basin of Jordan using GIS, remote sensing and DRASTIC: Applied Geography, v. 23, p. 303-324.

Alcalá, F. J., and E. Custodio, 2008, Using the Cl/Br ratio as a tracer to identify the origin of salinity in aquifers in Spain and Portugal: Journal of Hydrology, v. 359, p. 189-207.

Allen, D., 2004, Sources of groundwater salinity on islands using 18O, 2H, and 34S: Groundwater, v. 42, p. 17-31.

Allen, D., D. Abbey, D. Mackie, R. Luzitano, and M. Cleary, 2002, Investigation of potential saltwater intrusion pathways in a fractured aquifer using an integrated geophysical, geological and geochemical approach: Journal of Environmental & Engineering Geophysics, v. 7, p. 19-36.

Allen, D., E. Liteanu, and D. Mackie, 2003, Geologic controls on the occurrence of saltwater intrusion in heterogeneous and fractured island aquifers, southwestern British Columbia, Canada: Second International Conference on Saltwater Intrusion and Coastal Aquifers–Monitoring, Modeling, and Management. Merida, Yucatan, Mexico.

Allen, M. R., V. R. Barros, J. Broome, W. Cramer, R. Christ, J. A. Church, L. Clarke, Q. Dahe, P. Dasgupta, and N. K. Dubash, 2014, IPCC fifth assessment synthesis report-climate change 2014 synthesis report.

Aller, L., 1985, DRASTIC: a standardized system for evaluating ground water pollution potential using hydrogeologic settings, Robert S. Kerr Environmental Research Laboratory, Office of Research and Development, US Environmental Protection Agency

Aronsson, J., 2013, Saltvattenpåverkan i enskilda brunnar i kustnära områden: En undersökning av grundvattenförhållandena och riskerna för saltvattenpåverkan i S: t Annas skärgård, Östergötland.

Badaruddin, S., A. D. Werner, and L. K. Morgan, 2015, Water table salinization due to seawater intrusion: Water Resources Research, v. 51, p. 8397-8408.

Badaruddin, S., A. D. Werner, and L. K. Morgan, 2017, Characteristics of active seawater intrusion: Journal of Hydrology, v. 551, p. 632-647.

Balia, R., E. Gavaudo, F. Ardau, and G. Ghiglieri, 2003, Geophysical approach to the environmental study of a coastal plain: Geophysics, v. 68, p. 1446-1459.

Banks, D., N. E. Odling, H. Skarphagen, and E. Rohr-Torp, 1996, Permeability and stress in crystalline rocks: Terra Nova, v. 8, p. 223-235.

Banzhaf, S., L. L. Ekström, A. Ljungkvist, M. Granberg, J. Merisalu, S. Pokorny, and R. Barthel, 2017, Groundwater management in coastal zones and on islands in crystalline bedrock areas of Sweden: EGU General Assembly Conference Abstracts, p. 9401.

Barlow, P. M., 2003, Ground Water in fresh water-salt water environments of the Atlantic, v. 1262, Geological Survey (USGS).

Barlow, P. M., and E. G. Reichard, 2010, Saltwater intrusion in coastal regions of North America: Hydrogeology Journal, v. 18, p. 247-260.

Barthel, R., L. L. Ekström, A. Ljungkvist, M. Granberg, J. Merisalu, S. Pokorny, and S. Banzhaf, 2017, Combining scientific and societal challenges: a water supply case study from the Koster Islands, Sweden: EGU General Assembly Conference Abstracts, p. 9294.

Bear, J., 1979, Groundwater hydraulics, McGraw-Hill, New York.

Bear, J., A. H.-D. Cheng, S. Sorek, D. Ouazar, and I. Herrera, 1999, Seawater intrusion in coastal aquifers: concepts, method, and practices, v. 14, Springer Science & Business Media.

Bein, A., and A. Arad, 1992, Formation of saline groundwaters in the Baltic region through freezing of seawater during glacial periods: Journal of Hydrology, v. 140, p. 75-87.

Black, J. H., N. D. Woodman, and J. A. Barker, 2017, Groundwater flow into underground openings in fractured crystalline rocks: an interpretation based on long channels: Hydrogeology Journal, v. 25, p. 445-463.

Blakely, R. J., 1996, Potential theory in gravity and magnetic applications, Cambridge university press.

Bobba, A. G., 2002, Numerical modeling of salt-water intrusion due to human activities and sea-level change in the Godavari Delta, India: Hydrological Sciences Journal, v. 47, p. S67-S80.

Bohidar, R. N., J. P. Sullivan, and J. F. Hermance, 2001, Delineating depth to bedrock beneath shallow unconfined aquifers: a gravity transect across the Palmer river basin: Groundwater, v. 39, p. 729-736.

Boman, D., and G. Hanson, 2004, Salt grundvatten i Stockholms läns kust-och skärgårdsområden: metodik för miljöövervakning och undersökningsresultat 2003, Länsstyrelsen i Stockholms län.

Boman, D., Hansson, G, 2004, Salt grundvatten i Stockholms läns kust- och skärgårdsområden.

Caine, J. S., J. P. Evans, and C. B. Forster, 1996, Fault zone architecture and permeability structure: Geology, v. 24, p. 1025-1028.

Cashman, A., L. Nurse, and C. John, 2010, Climate change in the Caribbean: the water management implications: The Journal of Environment & Development, v. 19, p. 42-67.

Chang, S. W., T. P. Clement, M. J. Simpson, and K.-K. Lee, 2011, Does sea-level rise have an impact on saltwater intrusion?: Advances in water resources, v. 34, p. 1283-1291.

Choudhury, K., D. Saha, and P. Chakraborty, 2001, Geophysical study for saline water intrusion in a coastal alluvial terrain: Journal of applied geophysics, v. 46, p. 189-200.

Comte, J. C., C. Wilson, U. Ofterdinger, and A. González-Quirós, 2017, Effect of volcanic dykes on coastal groundwater flow and saltwater intrusion: A field-scale multiphysics approach and parameter evaluation: Water Resources Research, v. 53, p. 2171-2198.

Cooper, H. H., 1964, Seawater in coastal aquifers, US Government Printing Office.

Custodio, E., 2010, Coastal aquifers of Europe: an overview: Hydrogeology Journal, v. 18, p. 269-280.

Custodio, E., and G. Bruggeman, 1987, Groundwater problems in coastal areas: Studies and reports in hydrology (UNESCO).

Dahlin, T., and B. Zhou, 2004, A numerical comparison of 2D resistivity imaging with 10 electrode arrays: Geophysical prospecting, v. 52, p. 379-398.

Davis, S. N., J. T. Fabryka-Martin, and L. E. Wolfsberg, 2004, Variations of bromide in potable groundwater in the United States: Ground Water, v. 42, p. 902.

Delsman, J. R., E. S. Van Baaren, B. Siemon, W. Dabekaussen, M. C. Karaoulis, P. S. Pauw, T. Vermaas, H. Bootsma, P. G. De Louw, and J. L. Gunnink, 2018, Large-scale, probabilistic salinity mapping using airborne electromagnetics for groundwater management in Zeeland, the Netherlands: Environmental Research Letters, v. 13, p. 084011.

Denny, S., D. Allen, and J. Journeay, 2007, DRASTIC-Fm: a modified vulnerability mapping method for structurally controlled aquifers in the southern Gulf Islands, British Columbia, Canada: Hydrogeology Journal, v. 15, p. 483.

Dogan, M., R. L. Van Dam, G. Liu, M. M. Meerschaert, J. J. Butler, G. C. Bohling, D. A. Benson, and D. W. Hyndman, 2014, Predicting flow and transport in highly heterogeneous alluvial aquifers: Geophysical Research Letters, v. 41, p. 7560-7565.

Doughty, C., C.-F. Tsang, J.-E. Rosberg, C. Juhlin, P. F. Dobson, and J. T. Birkholzer, 2017, Flowing fluid electrical conductivity logging of a deep borehole during and following drilling: estimation of transmissivity, water salinity and hydraulic head of conductive zones: Hydrogeology Journal, v. 25, p. 501-517.

Duque, C., M. L. Calvache, A. Pedrera, W. Martín-Rosales, and M. López-Chicano, 2008, Combined time-domain electromagnetic soundings and gravimetry to determine marine intrusion in a detrital coastal aquifer (Southern Spain): Journal of Hydrology, v. 349, p. 536-547.

Earon, R., S. E. Dehkordi, and B. Olofsson, 2015, Groundwater Resources Potential in Hard Rock Terrain: A Multivariate Approach: Groundwater, v. 53, p. 748-758.

Ebert, K., K. Ekstedt, and J. Jarsjö, 2016, GIS analysis of effects of future Baltic sea level rise on the island of Gotland, Sweden: Natural Hazards & Earth System Sciences, v. 16.

Eliasson, T., 2011: Berggrundskarta, Kosterhavet Geoturistkarta, Dokumentation av de Svenska Nationalparkerna Nr 26. Naturvårdsverket och Sveriges geologiska undersökning.

Engard, B. R., C. D. McElwee, J. Healey, and R. Devlin, 2005, Hydraulic Tomography and High-Resolution Slug Testing to Determine Hydraulic Conductivity Distributions-Year 1, KANSAS UNIV LAWRENCE DEPT OF GEOLOGY.

Eriksson, M., K. Ebert, and J. Jarsjö, 2018, Well Salinization Risk and Effects of Baltic Sea Level Rise on the Groundwater-Dependent Island of Öland, Sweden: Water, v. 10, p. 141.

Essink, G. H. O., 2001, Improving fresh groundwater supply—problems and solutions: Ocean & Coastal Management, v. 44, p. 429-449.

Ferguson, G., and T. Gleeson, 2012, Vulnerability of coastal aquifers to groundwater use and climate change: Nature Climate Change, v. 2, p. 342.

Fetter, C. W., 2001, Applied hydrogeology: New Jersey: Upper Saddle River, p. 598.

Fetter, C., 1973, Water resources management in coastal plain aquifers: In Water For The Human Environment, Volume 1, Congress Papers.

FitzGerald, D. M., M. S. Fenster, B. A. Argow, and I. V. Buynevich, 2008, Coastal impacts due to sea-level rise: Annual Review of Earth and Planetary Sciences, v. 36.

Follin, S., and M. Stigsson, 2014, A transmissivity model for deformation zones in fractured crystalline rock and its possible correlation to in situ stress at the proposed high-level nuclear waste repository site at Forsmark, Sweden: Hydrogeology Journal, v. 22, p. 299-311.

Ford, A., & Blenkinsop, T. G. (2008). Evaluating geological complexity and complexity gradients as controls on copper mineralisation, Mt Isa Inlier. Australian Journal of Earth Sciences, 55(1), 13-23.

Freeze, R. A., and J. A. Cherry, 1979, Physical properties and principles: Groundwater; Prentice-Hall Inc.: Englewood Cliffs, NJ, USA, p. 14-79.

Gentry, W. M., and T. J. Burbey, 2004, Characterization Of Ground Water Flow From Spring Discharge In A Crystalline Rock Environment 1: Jawra Journal of the American Water Resources Association, v. 40, p. 1205-1217.

Gewers, K., and P. Håkansson, 1988, Saltvatteninträngning i brunnar i kusträra områden.

Ghyben, B. W., 1888, Nota in verband met de voorgenomen putboring nabij, Amsterdam: The Hague, v. 21.

Gilgallon, K., and M. McGivern, 2018, The use of Airborne EM to investigate coastal carbonate aquifer, seawater intrusions and sustainable borefield yield at Exmouth, Western Australia: ASEG Extended Abstracts, v. 2018, p. 1-6.

Guérin, R., M. Descloitres, A. Coudrain, A. Talbi, and R. Gallaire, 2001, Geophysical surveys for identifying saline groundwater in the semi-arid region of the central Altiplano, Bolivia: Hydrological processes, v. 15, p. 3287-3301.

Hageskov, B., 1985, Constrictional deformation of the Koster dyke swarm in a ductile sinistral shear zone, Koster Islands, SW Sweden: Bulletin of the Geological Society of Denmark, v. 34, p. 151-197.

Han, D., V. E. Post, and X. Song, 2015, Groundwater salinization processes and reversibility of seawater intrusion in coastal carbonate aquifers: Journal of Hydrology, v. 531, p. 1067-1080.

Herzberg, A., 1901, DieWasserversorgung einiger Nordseeber (The water supply of parts of the North Sea coast in Germany): Z: Gasbeleucht Wasserversorg.

Himi, M., J. Tapias, S. Benabdelouahab, A. Salhi, L. Rivero, M. Elgettafi, A. El Mandour, J. Stitou, and A. Casas, 2017, Geophysical characterization of saltwater intrusion in a coastal aquifer: The case of Martil-Alila plain (North Morocco): Journal of African Earth Sciences, v. 126, p. 136-147.

Hinze, W. J., 1990, The role of gravity and magnetic methods in engineering and environmental studies, Geotechnical an Environmental Geophysics: Volume I: Review and Tutorial, Society of Exploration Geophysicists, p. 75-126.

Hjerne, C., and R. Nordqvist, 2014, Relation between mass balance aperture and hydraulic properties from field experiments in fractured rock in Sweden: Hydrogeology Journal, v. 22, p. 1285-1292.

Hodgkinson, J., M. Cox, and S. McLoughlin, 2007, Groundwater mixing in a sand-island freshwater lens: density-dependent flow and stratigraphic controls: Australian Journal of Earth Sciences, v. 54, p. 927-946.

Hodkiewicz, P. F., Weinberg, R. F., Gardoll, S. J., & Groves, D. I. (2005). Complexity gradients in the Yilgarn Craton: fundamental controls on crustal-scale fluid flow and the formation of world-class orogenic-gold deposits. Australian Journal of Earth Sciences, 52(6), 831-841.

Holding, S., and D. Allen, 2015, From days to decades: numerical modeling of freshwater lens response to climate change stressors on small low-lying islands: Hydrology and Earth System Sciences, v. 19, p. 933-949.

Holding, S., and D. M. Allen, 2016, Risk to water security for small islands: an assessment framework and application: Regional environmental change, v. 16, p. 827-839.

Huyakorn, P. S., P. F. Andersen, J. W. Mercer, and H. O. White, 1987, Saltwater intrusion in aquifers: Development and testing of a three-dimensional finite element model: Water Resources Research, v. 23, p. 293-312.

Jørgensen, N. O., M. S. Andersen, and P. Engesgaard, 2008, Investigation of a dynamic seawater intrusion event using strontium isotopes (87Sr/86Sr): Journal of hydrology, v. 348, p. 257-269.

Kanagaraj, G., L. Elango, S. Sridhar, and G. Gowrisankar, 2018, Hydrogeochemical processes and influence of seawater intrusion in coastal aquifers south of Chennai, Tamil Nadu, India: Environmental Science and Pollution Research, v. 25, p. 8989-9011.

Katz, B. G., S. M. Eberts, and L. J. Kauffman, 2011, Using Cl/Br ratios and other indicators to assess potential impacts on groundwater quality from septic systems: a review and examples from principal aquifers in the United States: Journal of Hydrology, v. 397, p. 151-166.

Kennedy, G. W. (2012). Development of a GIS-based approach for the assessment of relative seawater intrusion vulnerability in Nova Scotia, Canada. IAH 2012.

Kim, K.-Y., Y.-S. Park, G.-P. Kim, and K.-H. Park, 2009, Dynamic freshwater–saline water interaction in the coastal zone of Jeju Island, South Korea: Hydrogeology Journal, v. 17, p. 617-629.

Kirkegaard, C., T. O. Sonnenborg, E. Auken, and F. Jørgensen, 2011, Salinity distribution in heterogeneous coastal aquifers mapped by airborne electromagnetics: Vadose Zone Journal, v. 10, p. 125-135.

Klassen, J., and D. Allen, 2017, Assessing the risk of saltwater intrusion in coastal aquifers: Journal of Hydrology, v. 551, p. 730-745.

Klassen, J., D. Aleen, and D. Kirtse, 2014, Chemical Indicators of Saltwater Intrusion for the Gulf Islands, British Columbia: Final Report, Department of Earth Sciences, Simon Rfaser University.

Kløve, B., H. M. L. Kvitsand, T. Pitkänen, M. J. Gunnarsdottir, S. Gaut, S. M. Gardarsson, P. M. Rossi, and I. Miettinen, 2017, Overview of groundwater sources and water-supply systems, and associated microbial pollution, in Finland, Norway and Iceland: Hydrogeology Journal, v. 25, p. 1033-1044.

Lång, L.-O.,B. Olofsson,E.Mellqvist,L.Ojala, L. Maxe, and M. Thorsbrink, 2006, Miljömålsuppföljning avgrundvatten ikustområden–statusbeskrivning ochdiskussionsunderlag.

Langman, J. B., and A. S. Ellis, 2010, A multi-isotope (δD, δ18O, 87Sr/86Sr, and δ11B) approach for identifying saltwater intrusion and resolving groundwater evolution along the Western Caprock Escarpment of the Southern High Plains, New Mexico: Applied Geochemistry, v. 25, p. 159-174.

Lara, K., and B. Weber, 2010, Evaluation of seawater intrusion using Sr isotopes: An example from Ensenada, BC, México, Water-Rock Interaction XIII, CRC Press, p. 96-99.

Lars Nordberg (1981) Problems in Sweden with intruded and fossil groundwater of marine origin. SWIM 7:4–5

Le Borgne, T., O. Bour, F. Paillet, and J.-P. Caudal, 2006, Assessment of preferential flow path connectivity and hydraulic properties at single-borehole and cross-borehole scales in a fractured aquifer: Journal of Hydrology, v. 328, p. 347-359.

Lindberg, J., B. Olofsson, and T. Gumbricht, 1996, Risk mapping of groundwater salinization using Geographical Information Systems: 14th Salt Water Intrusion Meeting (SWIM-96). Swedish Geological Survey (SGU) Reports and notes, p. 188-197.

Lindewald H (1981) Saline groundwater in Sweden. SWIM 7:24–32

Lindewald, H., 1981, Saline groundwater in Sweden: Intruded and relict groundwater of marine origin, 7th Salt-Water Intrusion Meeting, p. 24-32.

Llopis-Albert, C., and J. Capilla, 2010, Stochastic inverse modeling of hydraulic conductivity fields taking into account independent stochastic structures: A 3D case study: Journal of hydrology, v. 391, p. 277-288.

Lundqvist, J., 1986, Late Weichselian glaciation and deglaciation in Scandinavia: Quaternary Science Reviews, v. 5, p. 269-292.

Lundqvist, T., 1979, The precambrian of Sweden, Sveriges geologiska undersökning.

Lyles, J., 2000, Is seawater intrusion affecting groundwater on Lopez Island, Washington. USGS Numbered Series: US Geological Survey. Fact sheet FS-057-00.

Magnusson, N., 1963, In Magnusson, NH, Lundqvist, G. & Regnell, G: Sveriges geologi.

Mahesha, A., 1995, Parametric studies on the advancing interface in coastal aquifers due to linear variation of the freshwater level: Water Resources Research, v. 31, p. 2437-2442.

Masson-Delmotte, V., P. Zhai, H. Pörtner, D. Roberts, J. Skea, P. Shukla, A. Pirani, Y. Chen, S. Connors, and M. Gomis, 2018, IPCC, 2018: Summary for Policymakers: Global Warming of, v. 1.

Moir, R., A. Parker, and R. Bown, 2014, A simple inverse method for the interpretation of pumped flowing fluid, electrical conductivity logs: Water Resources Research, v. 50, p. 6466-6478.

Morgan, L. K., and A. D. Werner, 2015, A national inventory of seawater intrusion vulnerability for Australia: Journal of Hydrology: Regional Studies, v. 4, p. 686-698.

Naiman, R. J., J. J. Magnuson, D. M. McKnight, J. A. Stanford, and J. R. Karr, 1995, Freshwater ecosystems and their management: a national initiative: Science, v. 270, p. 584-585.

Neshat, A., B. Pradhan, S. Pirasteh, and H. Z. M. Shafri, 2014, Estimating groundwater vulnerability to pollution using a modified DRASTIC model in the Kerman agricultural area, Iran: Environmental earth sciences, v. 71, p. 3119-3131.

Neuman, S. P., 2005, Trends, prospects, and challenges in quantifying flow and transport through fractured rocks: Hydrogeology Journal, v. 13, p. 124-147.

Nowroozi, A. A., S. B. Horrocks, and P. Henderson, 1999, Saltwater intrusion into the freshwater aquifer in the eastern shore of Virginia: a reconnaissance electrical resistivity survey: Journal of Applied Geophysics, v. 42, p. 1-22.

Nyström, F., and K. Wall, 1993, Grundvattenprospektering på Nordkoster, Strömstads kommun.

Oki, D. S., W. R. Souza, E. L. Bolke, and G. R. Bauer, 1998, Numerical analysis of the hydrogeologic controls in a layered coastal aquifer system, Oahu, Hawaii, USA: Hydrogeology Journal, v. 6, p. 243-263.

Olofsson, B., 2005, Groundwater under Threat. The Swedish Research Council Formas Report. https://www.formas.se/download/18.462d60ec167c69393b91dfda/1549956094046/groundwater_under_threat.pdf accessed in 2019.

Panagopoulos, G., A. Antonakos, and N. Lambrakis, 2006, Optimization of the DRASTIC method for groundwater vulnerability assessment via the use of simple statistical methods and GIS: Hydrogeology Journal, v. 14, p. 894-911.

Park, H.-Y., K. Jang, J. W. Ju, and I. W. Yeo, 2012, Hydrogeological characterization of seawater intrusion in tidally-forced coastal fractured bedrock aquifer: Journal of hydrology, v. 446, p. 77-89.

Peternell, M., M. F. Bitencourt, and J. H. Kruhl, 2011, Combined quantification of anisotropy and inhomogeneity of magmatic rock fabrics–An outcrop scale analysis recorded in high resolution: Journal of Structural Geology, v. 33, p. 609-623.

Pinder, G. F., and H. H. Cooper Jr, 1970, A numerical technique for calculating the transient position of the saltwater front: Water Resources Research, v. 6, p. 875-882.

Post, V. E., G. O. Essink, A. Szymkiewicz, M. Bakker, G. Houben, E. Custodio, and C. Voss, 2018, Celebrating 50 years of SWIMs (Salt Water Intrusion Meetings): Hydrogeology Journal, v. 26, p. 1767-1770.

Post, V., 2005, Fresh and saline groundwater interaction in coastal aquifers: is our technology ready for the problems ahead?: Hydrogeology Journal, v. 13, p. 120-123.

Poulsen, S. E., K. R. Rasmussen, N. B. Christensen, and S. Christensen, 2010, Evaluating the salinity distribution of a shallow coastal aquifer by vertical multielectrode profiling (Denmark): Hydrogeology Journal, v. 18, p. 161-171.

Qian, H., P. Li, K. W. Howard, C. Yang, and X. Zhang, 2012, Assessment of groundwater vulnerability in the Yinchuan Plain, Northwest China using OREADIC: Environmental monitoring and assessment, v. 184, p. 3613-3628.

Rahman, A., 2008, A GIS based DRASTIC model for assessing groundwater vulnerability in shallow aquifer in Aligarh, India: Applied geography, v. 28, p. 32-53.

Ranjan, P., S. Kazama, M. Sawamoto, and A. Sana, 2009, Global scale evaluation of coastal fresh groundwater resources: Ocean & Coastal Management, v. 52, p. 197-206.

Reilly, T. E., and A. S. Goodman, 1985, Quantitative analysis of saltwater-freshwater relationships in groundwater systems—a historical perspective: Journal of Hydrology, v. 80, p. 125-160.

Rupert, M., 2001, Calibration of the DRASTIC groundwater vulnerability mapping method: Groundwater, v. 39, p. 625-630.

Sanford, W. E., and J. P. Pope, 2010, Current challenges using models to forecast seawater intrusion: lessons from the Eastern Shore of Virginia, USA: Hydrogeology Journal, v. 18, p. 73-93.

Scheiber, T., O. Fredin, G. Viola, A. Jarna, D. Gasser, and R. Łapińska-Viola, 2015, Manual extraction of bedrock lineaments from high-resolution LiDAR data: methodological bias and human perception: GFF, v. 137, p. 362-372.

Siemon, B., A. V. Christiansen, and E. Auken, 2009, A review of helicopter-borne electromagnetic methods for groundwater exploration: Near Surface Geophysics, v. 7, p. 629-646.

Small, C., and R. J. Nicholls, 2003, A global analysis of human settlement in coastal zones: Journal of coastal research, p. 584-599.

Snow, D. T., 1969, Anisotropie permeability of fractured media: Water Resources Research, v. 5, p. 1273-1289.

Stewart, M. T., 1982; Evaluation of electromagnetic methods for rapid mapping of salt-water interfaces in coastal aquifers: Groundwater, v. 20, p. 538-545.

Sund B, Bergman G (1981) Seawater intrusion in drilled wells. SWIM 7:45–58

Surrette, M.J. and Allen, D.M. (2008) Quantifying heterogeneity in variably fractured sedimentary rock using a hydrostructural domain. Geological Society of America Bulletin 120 (1-2), 225-237.

Surrette, M.J., Allen, D.M. and Journeay, M. (2008) Regional evaluation of hydraulic properties in

Susanne Liljenström and Karin Björk, 2013, National parks of Sweden, SBN 978-91-620-8412-7

Tangestani, M. H., 2009, A comparative study of Dempster–Shafer and fuzzy models for landslide susceptibility mapping using a GIS: An experience from Zagros Mountains, SW Iran: Journal of Asian Earth Sciences, v. 35, p. 66-73.

Thunqvist, E.-L., 2011, Enskilda brunnar och saltvatteninträngning på Ornö, KTH CHB.

Tsang, C.-F., J.-E. Rosberg, P. Sharma, T. Berthet, C. Juhlin, and A. Niemi, 2016, Hydrologic testing during drilling: application of the flowing fluid electrical conductivity (FFEC) logging method to drilling of a deep borehole.: Hydrogeology Journal, v. 24, p. 1333-1341.

Vengosh, A., and I. Pankratov, 1998, Chloride/bromide and chloride/fluoride ratios of domestic sewage effluents and associated contaminated ground water: Groundwater, v. 36, p. 815-824.

Vias, J., B. Andreo, M. Perles, and F. Carrasco, 2005, A comparative study of four schemes for groundwater vulnerability mapping in a diffuse flow carbonate aquifer under Mediterranean climatic conditions: Environmental Geology, v. 47, p. 586-595.

Vidstrand, P., S. Follin, J.-O. Selroos, and J.-O. Näslund, 2014, Groundwater flow modeling of periods with periglacial and glacial climate conditions for the safety assessment of the proposed high-level nuclear waste repository site at Forsmark, Sweden: Hydrogeology Journal, v. 22, p. 1251-1267.

Vidstrand, P., S. Follin, J.-O. Selroos, J.-O. Näslund, and I. Rhén, 2013, Modeling of groundwater flow at depth in crystalline rock beneath a moving ice-sheet margin, exemplified by the Fennoscandian Shield, Sweden: Hydrogeology Journal, v. 21, p. 239-255.

Viezzoli, A., L. Tosi, P. Teatini, and S. Silvestri, 2010, Surface water–groundwater exchange in transitional coastal environments by airborne electromagnetics: the Venice Lagoon example: Geophysical Research Letters, v. 37.

Voss, C. I., and W. R. Souza, 1987, Variable density flow and solute transport simulation of regional aquifers containing a narrow freshwater-saltwater transition zone: Water Resources Research, v. 23, p. 1851-1866.

Webb, M. D., and K. W. Howard, 2011, Modeling the transient response of saline intrusion to rising sea-levels: Groundwater, v. 49, p. 560-569.

Werner, A. D., 2017, On the classification of seawater intrusion: Journal of Hydrology, v. 551, p. 619-631.

Werner, A. D., and C. T. Simmons, 2009, Impact of sea-level rise on seawater intrusion in coastal aquifers: Groundwater, v. 47, p. 197-204.

Werner, A. D., and M. R. Gallagher, 2006, Characterisation of sea-water intrusion in the Pioneer Valley, Australia using hydrochemistry and three-dimensional numerical modeling: Hydrogeology Journal, v. 14, p. 1452-1469.

Werner, A. D., J. D. Ward, L. K. Morgan, C. T. Simmons, N. I. Robinson, and M. D. Teubner, 2012, Vulnerability indicators of seawater intrusion: Groundwater, v. 50, p. 48-58.

Werner, A. D., M. Bakker, V. E. Post, A. Vandenbohede, C. Lu, B. Ataie-Ashtiani, C. T. Simmons, and D. A. Barry, 2013, Seawater intrusion processes, investigation, and management: recent advances and future challenges: Advances in Water Resources, v. 51, p. 3-26.

Werner, A., and D. Lockington, 2004, The potential for soil salinization above aquifers impacted by seawater intrusion: Proceedings of 13th International Soil Conservation Organisation Conference: Conserving Soil and Water for Society: Sharing Solutions, p. 4-9.

West, L. J., and N. E. Odling, 2007, Characterization of a multilayer aquifer using open well dilution tests: Groundwater, v. 45, p. 74-84.

Wilson, T. P., and D. T. Long, 1993, Geochemistry and isotope chemistry of Michigan Basin brines: Devonian formations: Applied Geochemistry, v. 8, p. 81-100.

Yakirevich, A., A. Melloul, S. Sorek, S. Shaath, and V. Borisov, 1998, Simulation of seawater intrusion into the Khan Yunis area of the Gaza Strip coastal aquifer: Hydrogeology Journal, v. 6, p. 549-559.